



Lecture 44. Constituent Lidar (4)

Multi-wavelength Raman DIAL & DOAS and MAX-DOAS

- Review conventional DIAL
- Raman DIAL for Ozone Measurement
- Rotational Vibrational-Rotational (RVR) Raman DIAL
- Multiwavelength (Raman) DIAL
- Differential Optical Absorption Spectroscopy (DOAS)



Lidar Equation for DIAL

- DIAL lidar equation

$$P_S(\lambda, R) = P_L(\lambda) \left[\beta_{scatter}(\lambda, R) \Delta R \right] \left(\frac{A}{R^2} \right) \exp \left[-2 \int_0^R \bar{\alpha}(\lambda, r) dr \right]$$
$$\times \exp \left[-2 \int_0^R \sigma_{abs}(\lambda, r) n_c(r) dr \right] [\eta(\lambda) G(R)] + P_B$$

Extinction caused by interested constituent extinction (absorption)

Extinction caused by other molecules and aerosols

- Compared to resonance fluorescence, the main difference in DIAL is that the backscatter coefficient is from the elastic-scattering from air molecules and aerosols, not from the fluorescence of interested molecules.

$$\beta_{Scatter}(\lambda, R) = \beta_{aer}(\lambda, R) + \beta_{mol}(\lambda, R)$$

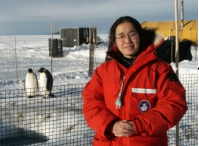
- The parameter in the DIAL equation

$$\bar{\alpha}(\lambda, r) = \alpha_{aer}(\lambda, r) + \alpha_{mol}(\lambda, r) + \sigma_{IG}(\lambda, r) n_{IG}(r)$$

Aerosol Extinction

Air Molecule Extinction

Interference gas absorption



Conventional DIAL Ozone Measurement

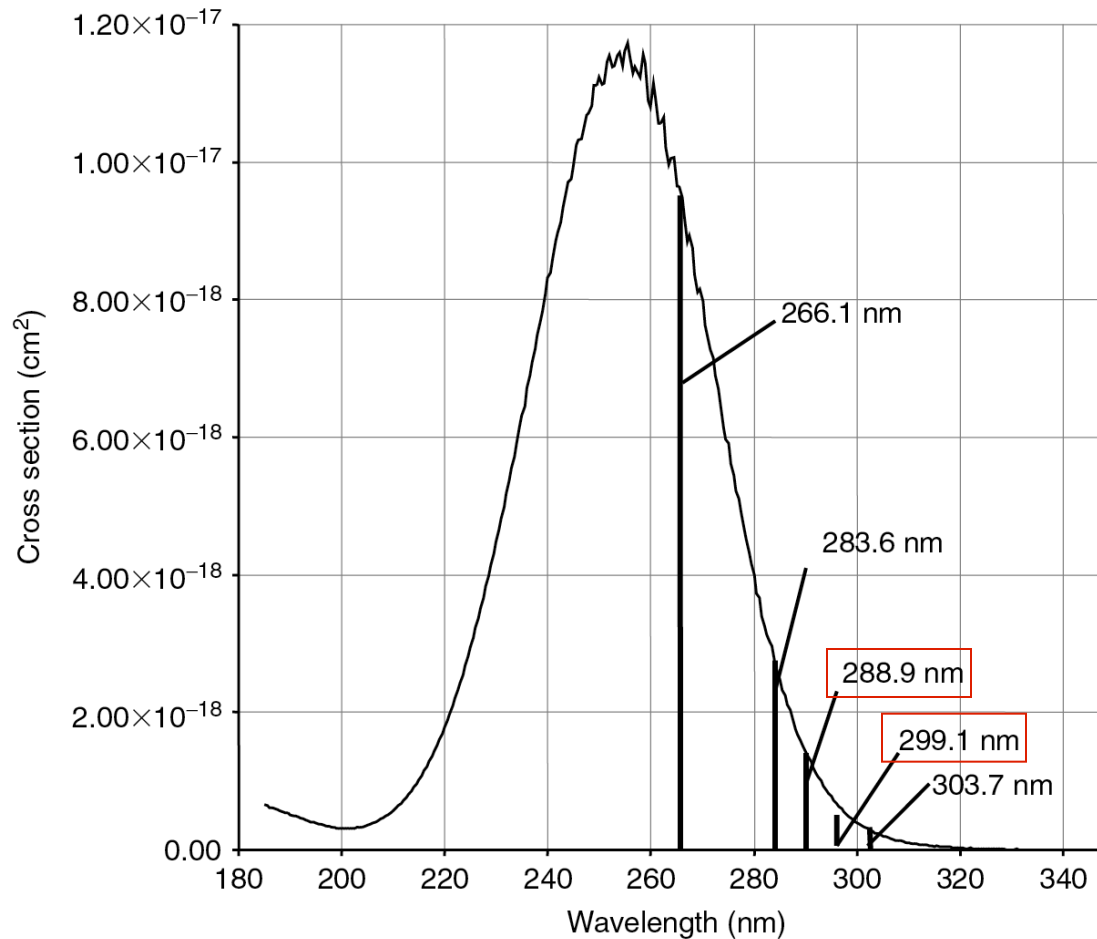
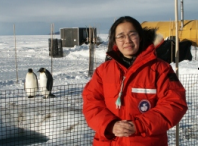


Figure 4.1 Ozone absorption spectrum in the UV: the Raman shifted wavelengths given in Table 4.2 are highlighted in this figure.

$$\lambda_{ON} = 288.9 \text{ nm}$$
$$\lambda_{OFF} = 299.1 \text{ nm}$$



Conventional DIAL Solutions

$$n_c(R) = \frac{1}{2\Delta\sigma_{abs}} \frac{d}{dR} \left\{ \ln \left[\frac{P_S(\lambda_{OFF}, R) - P_B}{P_S(\lambda_{ON}, R) - P_B} \right] \right. \\ \left. - \ln \left[\frac{P_L(\lambda_{OFF})\eta(\lambda_{OFF})}{P_L(\lambda_{ON})\eta(\lambda_{ON})} \right] \right. \\ \left. - \ln \left[\frac{\beta_{aer}(\lambda_{OFF}, R) + \beta_{mol}(\lambda_{OFF}, R)}{\beta_{aer}(\lambda_{ON}, R) + \beta_{mol}(\lambda_{ON}, R)} \right] \right\} \\ - \frac{1}{\Delta\sigma_{abs}} \left\{ \right. \\ \left. [\alpha_{aer}(\lambda_{ON}, R) - \alpha_{aer}(\lambda_{OFF}, R)] \right. \\ \left. + [\alpha_{mol}(\lambda_{ON}, R) - \alpha_{mol}(\lambda_{OFF}, R)] \right. \\ \left. + [\sigma_{IG}(\lambda_{ON}, R) - \sigma_{IG}(\lambda_{OFF}, R)] n_{IG} \right\}$$

All terms non-range dependent vanish after the derivative d/dR

Introducing large error when large aerosol gradient or IG exists⁴



Ozone Raman DIAL

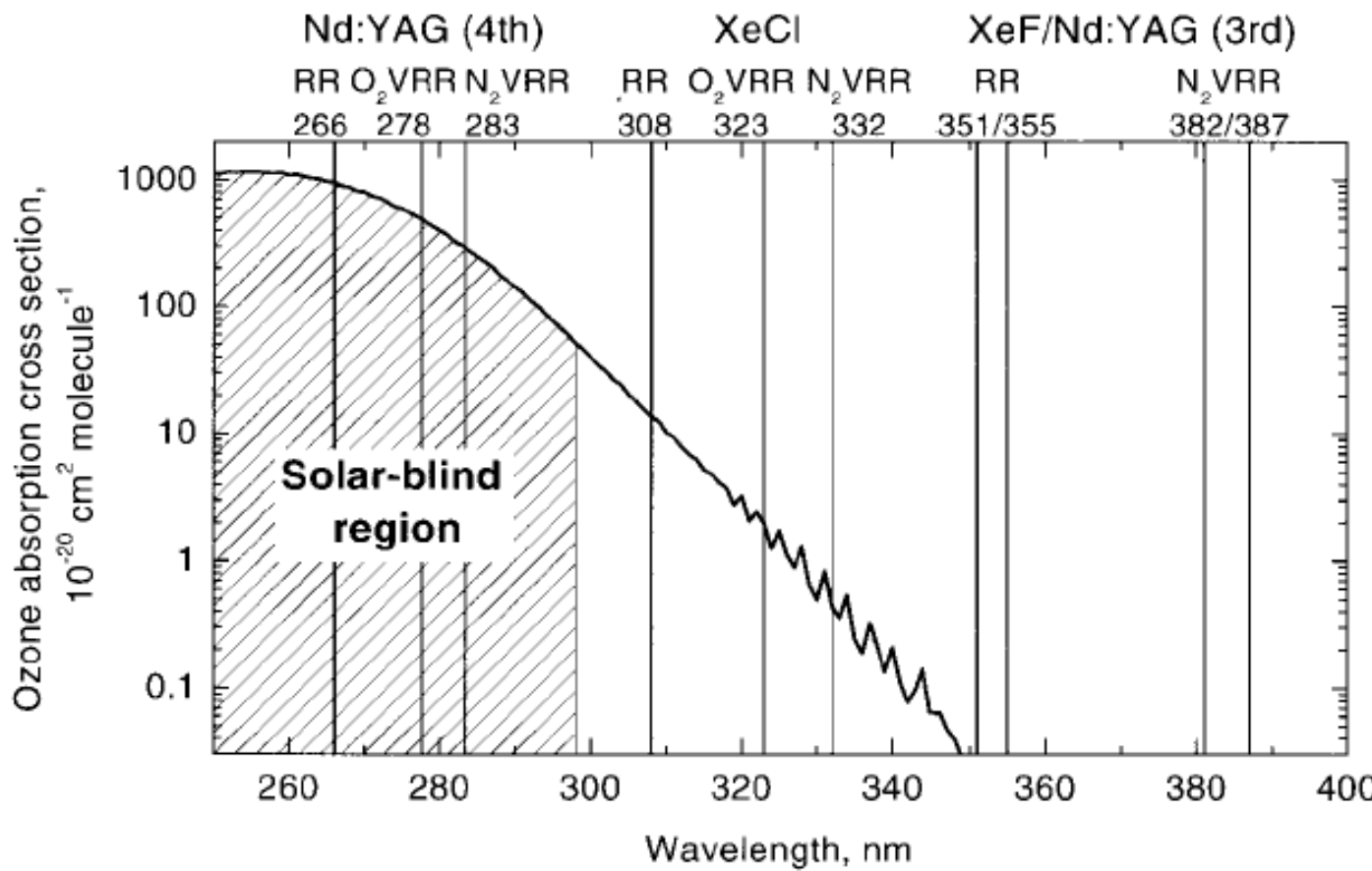
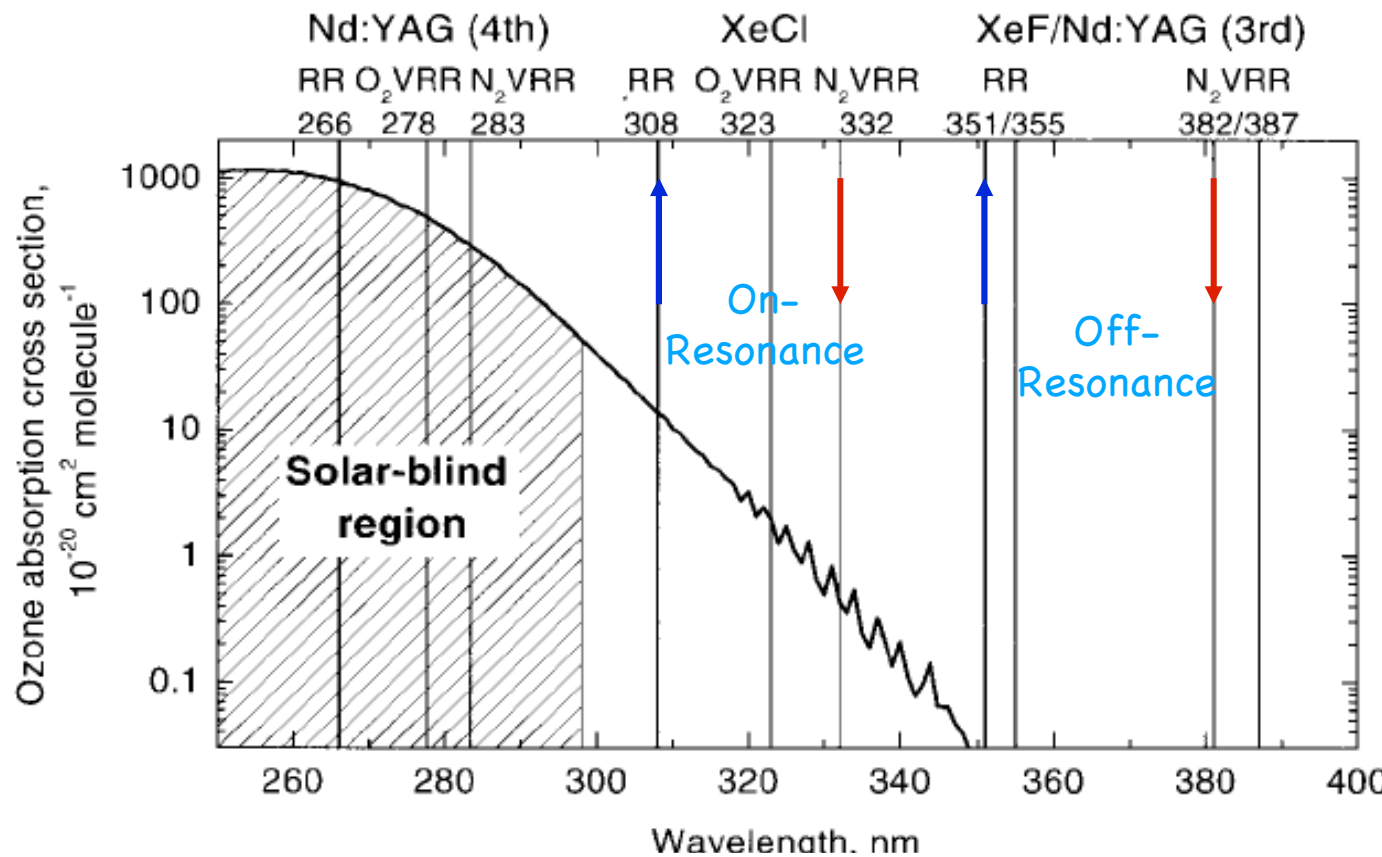


Fig. 9.5. Ozone absorption cross section and wavelengths applied in the ozone Raman DIAL technique for upper tropospheric and stratospheric measurements ($\lambda > 300 \text{ nm}$) and for boundary-layer measurements in the solar-blind region ($\lambda < 300 \text{ nm}$).



Conventional Raman DIAL for O_3 Measurements in Clouds



Conventional Raman DIAL uses two primary wavelengths transmitted (e.g., 308 and 351 nm) into the atmosphere and ozone is calculated from the differential absorption of the corresponding Raman return signals of molecular N_2 (e.g., 332 and 382 nm).



Raman DIAL Equations

- Raman channels (e.g., from N₂ Raman inelastic scattering, instead of elastic scattering from air molecules or aerosols),

$$\begin{aligned} P_S(\lambda_{\text{Ref}}^{ON}, R) = & P_L(\lambda_0^{ON}) \left[\beta_{Raman}(\lambda_0^{ON}, \lambda_{\text{Ref}}^{ON}, R) \Delta R \right] \left(\frac{A}{R^2} \right) \\ & \times \exp \left[- \int_0^R \left(\alpha_{aer}(\lambda_0^{ON}, r) + \alpha_{aer}(\lambda_{\text{Ref}}^{ON}, r) + \alpha_{mol}(\lambda_0^{ON}, r) + \alpha_{mol}(\lambda_{\text{Ref}}^{ON}, r) \right) dr \right] \\ & \times \exp \left[- \int_0^R \left(\sigma_{IG}(\lambda_0^{ON}, r) + \sigma_{IG}(\lambda_{\text{Ref}}^{ON}, r) \right) n_{IG} dr \right] \\ & \times \exp \left[- \int_0^R \left(\sigma_{abs}(\lambda_0^{ON}, r) + \sigma_{abs}(\lambda_{\text{Ref}}^{ON}, r) \right) n_c(r) dr \right] \left[\eta(\lambda_{\text{Ref}}^{ON}) G(R) \right] + P_B \end{aligned}$$

$$\begin{aligned} P_S(\lambda_{\text{Ref}}^{OFF}, R) = & P_L(\lambda_0^{OFF}) \left[\beta_{Raman}(\lambda_0^{OFF}, \lambda_{\text{Ref}}^{OFF}, R) \Delta R \right] \left(\frac{A}{R^2} \right) \\ & \times \exp \left[- \int_0^R \left(\alpha_{aer}(\lambda_0^{OFF}, r) + \alpha_{aer}(\lambda_{\text{Ref}}^{OFF}, r) + \alpha_{mol}(\lambda_0^{OFF}, r) + \alpha_{mol}(\lambda_{\text{Ref}}^{OFF}, r) \right) dr \right] \\ & \times \exp \left[- \int_0^R \left(\sigma_{IG}(\lambda_0^{OFF}, r) + \sigma_{IG}(\lambda_{\text{Ref}}^{OFF}, r) \right) n_{IG} dr \right] \\ & \times \exp \left[- \int_0^R \left(\sigma_{abs}(\lambda_0^{OFF}, r) + \sigma_{abs}(\lambda_{\text{Ref}}^{OFF}, r) \right) n_c(r) dr \right] \left[\eta(\lambda_{\text{Ref}}^{OFF}) G(R) \right] + P_B \end{aligned}$$



Solution for Raman DIAL Equations

- From the two Raman reference channel equations, we obtain the number density of the constituent that we are interested in

$$n_c(R) = \frac{1}{\Delta\sigma_{abs}} \frac{d}{dR} \left\{ \begin{array}{l} \ln \left[\frac{P_S(\lambda_{Ref}^{OFF}, R) - P_B}{P_S(\lambda_{Ref}^{ON}, R) - P_B} \right] \\ - \ln \left[\frac{P_L(\lambda_0^{OFF}) \eta(\lambda_{Ref}^{OFF})}{P_L(\lambda_0^{ON}) \eta(\lambda_{Ref}^{ON})} \right] \\ - \ln \left[\frac{\beta_{Raman}(\lambda_{Ref}^{OFF}, R)}{\beta_{Raman}(\lambda_{Ref}^{ON}, R)} \right] \\ - \frac{1}{\Delta\sigma_{abs}} \left\{ \begin{array}{l} \Delta\alpha_{aer}(R) \\ + \Delta\alpha_{mol}(R) \\ + \Delta\sigma_{IG}(R)n_{IG} \end{array} \right\} \end{array} \right\}$$

A
B
C
D
E
F

- Here, the Δ expressions consist of four terms each

$$\Delta\xi = \xi(\lambda_0^{ON}) + \xi(\lambda_{Ref}^{ON}) - \xi(\lambda_0^{OFF}) - \xi(\lambda_{Ref}^{OFF})$$

with

$$\xi = \sigma_{abs}, \alpha_{aer}, \alpha_{mol}, \sigma_{IG}$$



Solution in Ozone Case

- ❑ Term B can be measured and it is range-independent, so the derivative is zero,
- ❑ Term C is only concerned about molecule Raman scattering, so can be calculated.
- ❑ Term D will be determined through using the Raman channel at OFF wavelength and introducing Angstrom exponent.
- ❑ Term E is concerned about molecule Rayleigh scattering, so can be calculated from atmosphere temperature and pressure.
- ❑ Term F can be minimized through choosing proper wavelengths, thus, can be ignored.

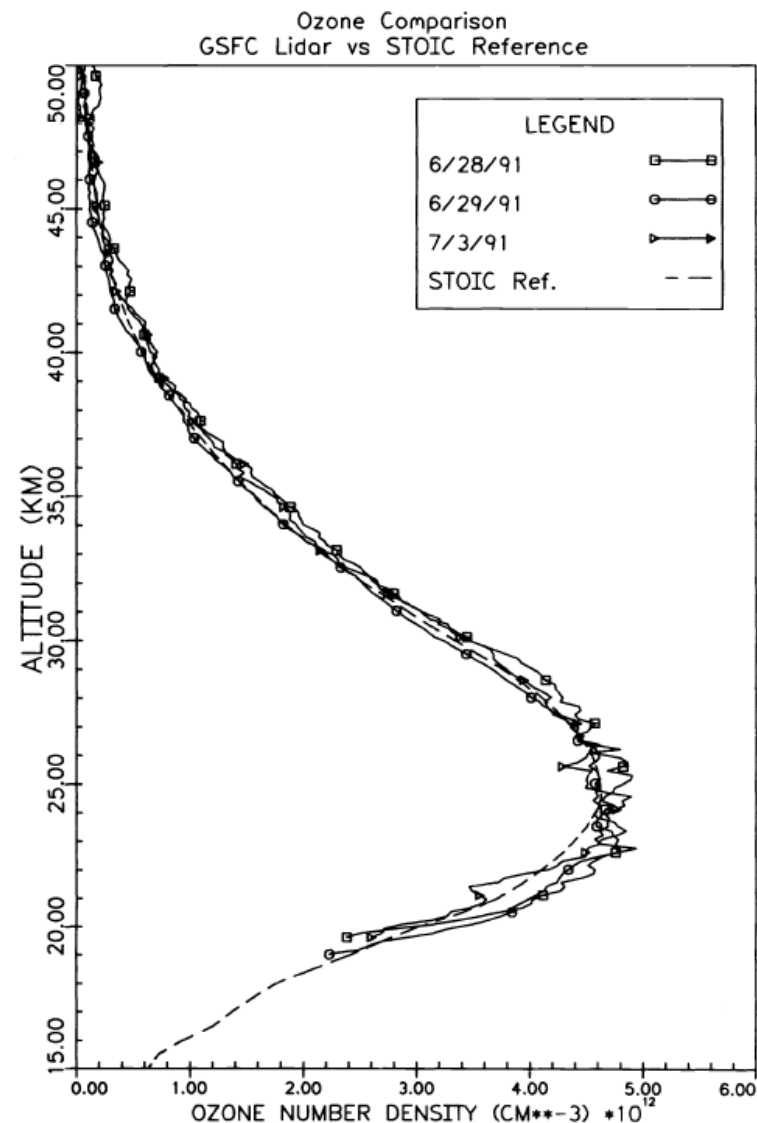
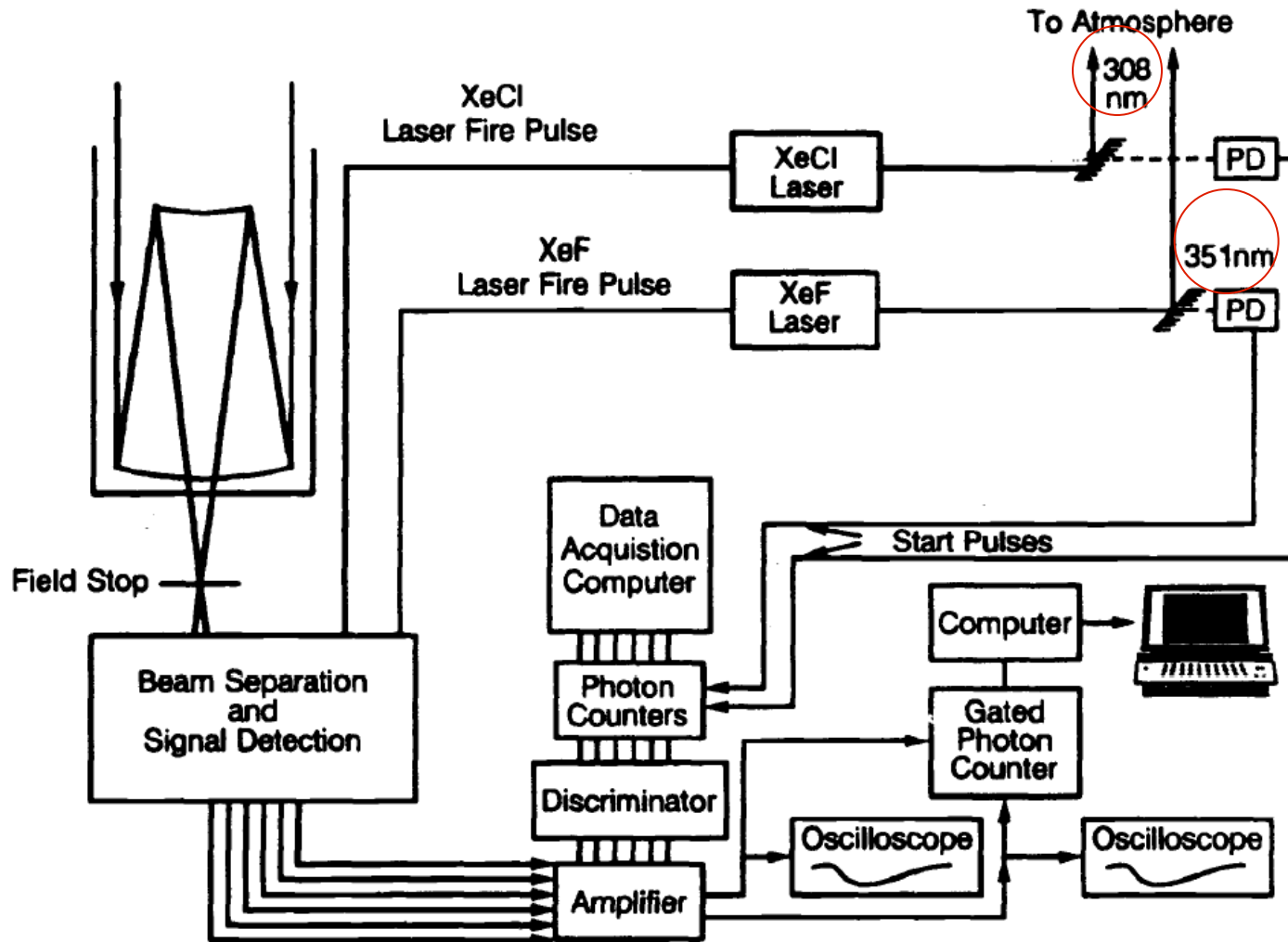


Fig. 6 GSFC lidar ozone profiles taken at JPL-TMO during June and July 1991 using the mechanical chopper.



Ozone Raman DIAL Instrumentation



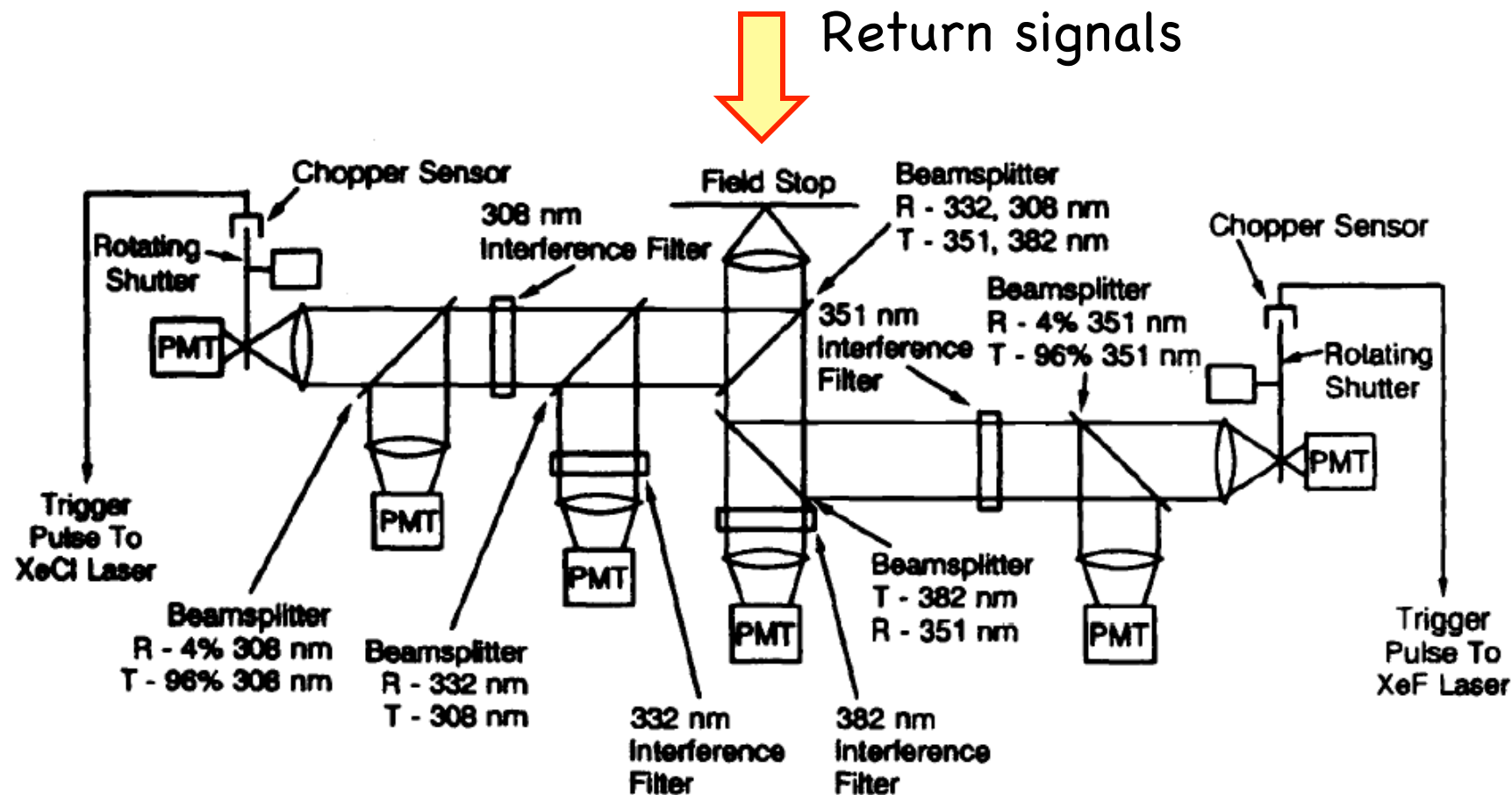
Return Signals -

On-line: 332 nm (N_2 Raman scattering from 308 nm)

Off-line: 382 nm (N_2 Raman scattering from 351 nm)

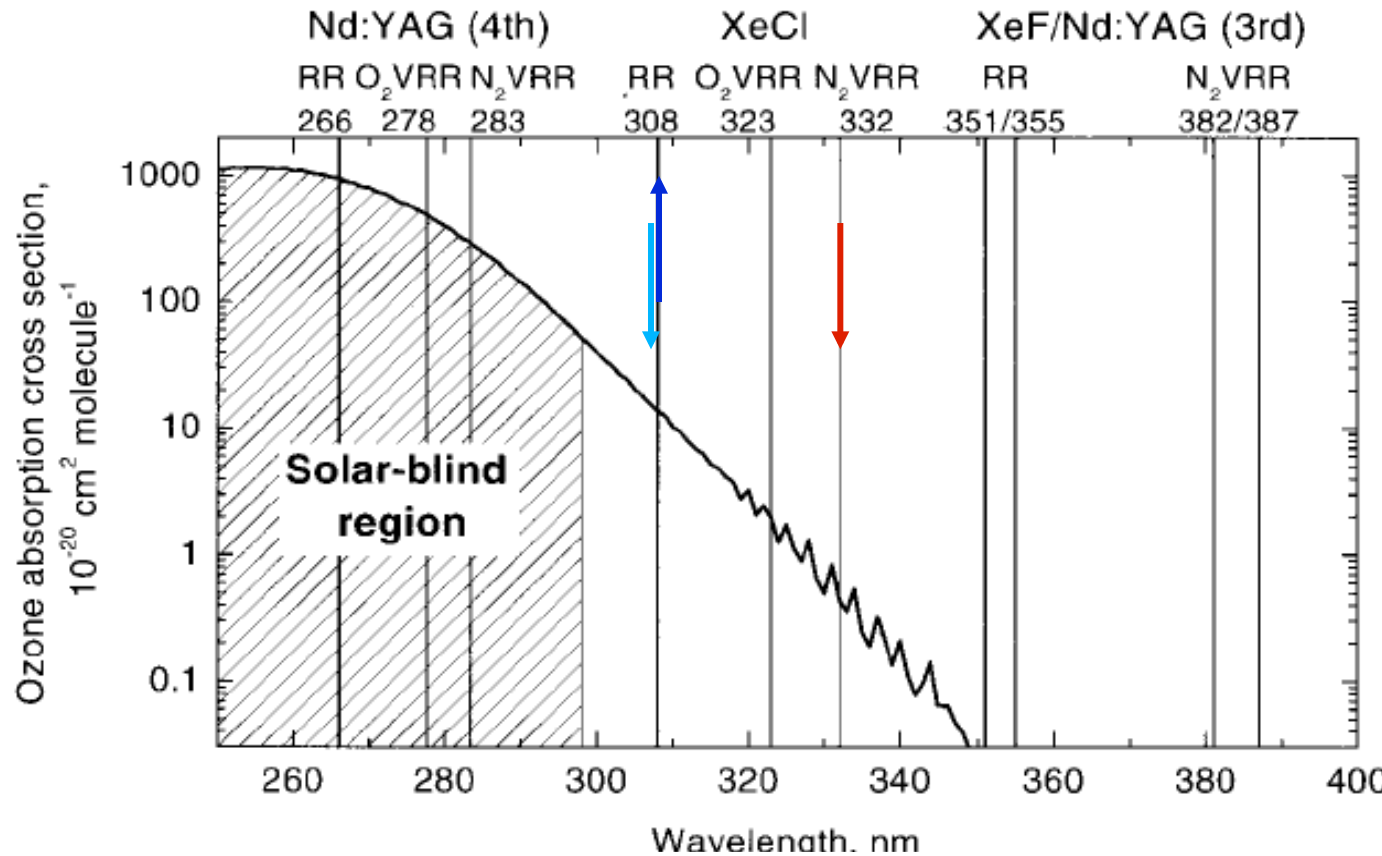


Ozone Raman DIAL Receiver





RVR Raman DIAL for O_3 Measurement



Rotational Vibrational-Rotational Raman DIAL transmits single primary wavelength (e.g., 308 nm) into the atmosphere and then ozone measurement is based on differential absorption of ozone between the purely rotational Raman (RR) return signals from N_2 (307 nm) and O_2 (307 nm) as the on-resonance wavelength, and the vibrational-rotational Raman (VRR) return signals from N_2 (332 nm) or O_2 (323 nm) as the off-resonance wavelength.



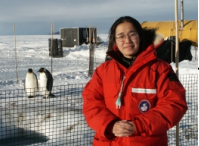
Rotational Vibrational-Rotational (RVR) Raman DIAL with Single Laser

Table 1. Parameters of the Conventional Raman DIAL and the RVR Raman DIAL's^a

Lidar	On-Resonance		Off-Resonance			$\Delta\lambda$ (nm)	$\Delta C_{O_3}^{abs}$ ($10^{-24} m^2$)
	Raman Wavelength (nm)	λ_L (nm)	Raman Wavelength (nm)	λ_L (nm)			
O ₂ RVR Raman DIAL	307	308	323	308		16	11.7
N ₂ RVR Raman DIAL	307	308	332	308		25	12.3
Raman DIAL	332	308	387	355		79	12.4

^a $\Delta\lambda$, maximum spectral separation of the signals used for the measurements. Differential ozone absorption cross sections ($\Delta C_{O_3}^{abs}$) are calculated from Ref. 13 ($T = 226$ K). Wavelength values are rounded to full nanometers.

The RVR Raman DIAL measurement yields the numbers $N(\lambda, z)$ of lidar return photons from distance z at the rotational Raman wavelength λ_R of molecular oxygen and nitrogen and at the vibrational-rotational Raman wavelength λ_{VR} of O₂ or N₂, if light of the primary wavelength λ_L is transmitted. When absorption by particles and trace gases other than ozone is neglected, a condition satisfied for cirrus measurements in the free troposphere,³ the RVR Raman DIAL ozone molecule number density $n(z)$ in the single-scattering approximation is given by



RVR Raman DIAL

$$n(z) = RVRN - RVRM - VRP, \quad (1)$$

where

$$RVRN = \frac{(d/dz)\ln[N(\lambda_{VR}, z)/N(\lambda_R, z)]}{C_{O_3}^{\text{abs}}(\lambda_R, T) - C_{O_3}^{\text{abs}}(\lambda_{VR}, T)},$$

$$RVRM = \frac{\alpha_{\text{mol}}^{\text{sca}}(\lambda_R, z) - \alpha_{\text{mol}}^{\text{sca}}(\lambda_{VR}, z)}{C_{O_3}^{\text{abs}}(\lambda_R, T) - C_{O_3}^{\text{abs}}(\lambda_{VR}, T)},$$

$$VRP = \frac{\alpha_{\text{par}}^{\text{sca}}(\lambda_R, z) - \alpha_{\text{par}}^{\text{sca}}(\lambda_{VR}, z)}{C_{O_3}^{\text{abs}}(\lambda_R, T) - C_{O_3}^{\text{abs}}(\lambda_{VR}, T)}.$$

Here $C_{O_3}^{\text{abs}}(\lambda, T)$ is the ozone absorption cross section at temperature T , and $\alpha_{\text{mol}}^{\text{sca}}(\lambda, z)$ and $\alpha_{\text{par}}^{\text{sca}}(\lambda, z)$ are the Rayleigh extinction and the single-scattering particle extinction coefficient, respectively. Similar expressions, RDN , RDM , and RDP , have been derived for conventional Raman DIAL.⁴

[Reichardt et al., Applied Optics, 39, 6072-6079, 2000]



Single-Laser RVR Raman DIAL

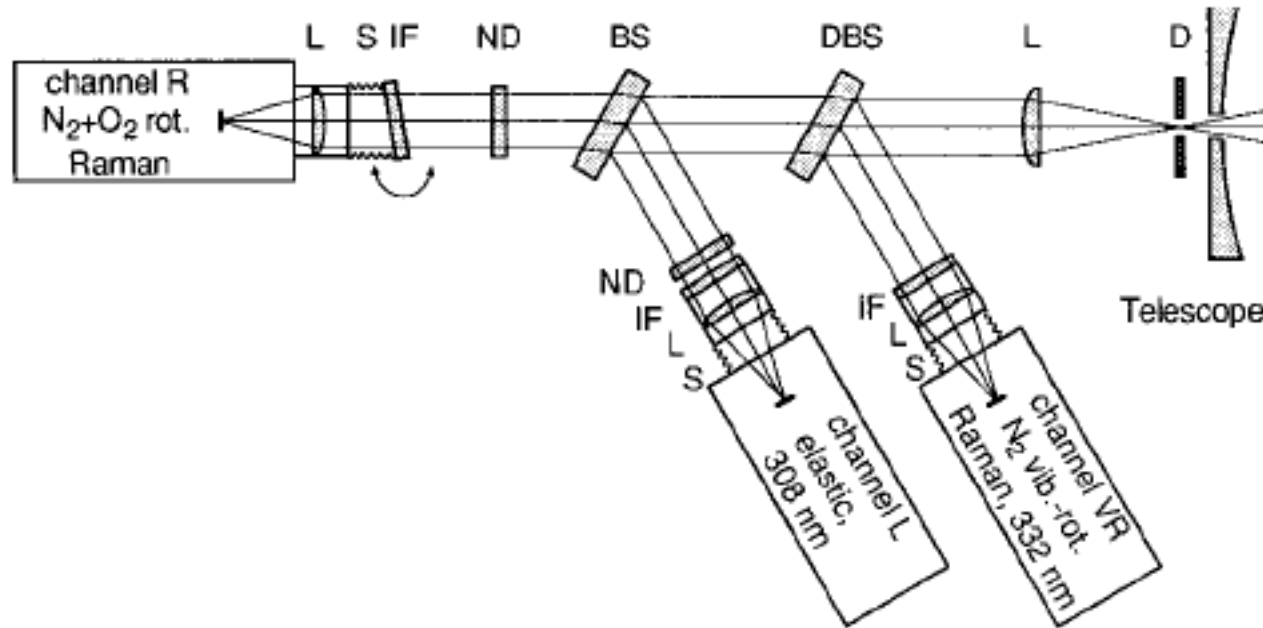


Fig. 3. RVR Raman DIAL receiver: D, diaphragm; L, lens; DBS, dichroic beam splitter; BS, beam splitter; ND, neutral-density filter; IF, interference filter; S, flexible shield. Atmospheric rotational Raman, elastic, and N₂ vibrational–rotational Raman backscattering signals are detected in channels R, L, and VR. The center wavelength of the channel-R interference filter can be tuned by rotating the filter around the vertical axis.



RVR Raman DIAL Equation

- For the elastic DIAL channel at ON-resonance wavelength 308 nm,

$$\begin{aligned} P_S(\lambda_L, R) = & P_L(\lambda_L) \left[(\beta_{aer}(\lambda_L, R) + \beta_{mol}(\lambda_L, R)) \Delta R \right] \left(\frac{A}{R^2} \right) \exp \left[-2 \int_0^R (\alpha_{aer}(\lambda_L, r) + \alpha_{mol}(\lambda_L, r)) dr \right] \\ & \times \exp \left[-2 \int_0^R \sigma_{IG}(\lambda_L, r) n_{IG} dr \right] \exp \left[-2 \int_0^R \sigma_{abs}(\lambda_L, r) n_c(r) dr \right] [\eta(\lambda_L) G(R)] + P_B \end{aligned}$$

- For the purely rotational Raman channels from N₂ and O₂ at 307 nm,

$$\begin{aligned} P_S(\lambda_{RR}, R) = & P_L(\lambda_L) [\beta_{Raman}(\lambda_L, \lambda_{RR}, R) \Delta R] \left(\frac{A}{R^2} \right) \\ & \times \exp \left[- \int_0^R (\alpha_{aer}(\lambda_L, r) + \alpha_{aer}(\lambda_{RR}, r) + \alpha_{mol}(\lambda_L, r) + \alpha_{mol}(\lambda_{RR}, r)) dr \right] \\ & \times \exp \left[- \int_0^R (\sigma_{IG}(\lambda_L, r) + \sigma_{IG}(\lambda_{RR}, r)) n_{IG} dr \right] \\ & \times \exp \left[- \int_0^R (\sigma_{abs}(\lambda_L, r) + \sigma_{abs}(\lambda_{RR}, r)) n_c(r) dr \right] [\eta(\lambda_{RR}) G(R)] + P_B \end{aligned}$$

The beauty of the RVR Raman DIAL is the utilization of pure rotational Raman (RR) scattering so that aerosol backscatter is excluded in the RR channel. ¹⁶



RVR Raman DIAL Equation Continued

- For the vibrational-rotational Raman channel from N₂ at 332 nm,

$$\begin{aligned} P_S(\lambda_{VRR}, R) = & P_L(\lambda_L) \left[\beta_{Raman}(\lambda_L, \lambda_{VRR}, R) \Delta R \right] \left(\frac{A}{R^2} \right) \\ & \times \exp \left[- \int_0^R (\alpha_{aer}(\lambda_L, r) + \alpha_{aer}(\lambda_{VRR}, r) + \alpha_{mol}(\lambda_L, r) + \alpha_{mol}(\lambda_{VRR}, r)) dr \right] \\ & \times \exp \left[- \int_0^R (\sigma_{IG}(\lambda_L, r) + \sigma_{IG}(\lambda_{VRR}, r)) n_{IG} dr \right] \\ & \times \exp \left[- \int_0^R (\sigma_{abs}(\lambda_L, r) + \sigma_{abs}(\lambda_{VRR}, r)) n_c(r) dr \right] [\eta(\lambda_{VRR}) G(R)] + P_B \end{aligned}$$

Certainly, the vibrational-rotational Raman (VRR) scattering channel also excludes aerosol backscatter.



Solution for RVR Raman DIAL

- From the Rotational Raman (RR) and the Vibrational-Rotational Raman (VRR) equations, the ozone number density can be derived as

$$n_c(R) = \frac{1}{\Delta\sigma_{abs}} \frac{d}{dR} \left\{ \begin{array}{l} \ln \left[\frac{P_S(\lambda_{VRR}, R) - P_B}{P_S(\lambda_{RR}, R) - P_B} \right] \\ - \ln \left[\frac{\eta(\lambda_{VRR})}{\eta(\lambda_{RR})} \right] \\ - \ln \left[\frac{\beta_{Raman}(\lambda_{VRR}, R)}{\beta_{Raman}(\lambda_{RR}, R)} \right] \\ - \frac{1}{\Delta\sigma_{abs}} \left\{ \begin{array}{l} \Delta\alpha_{aer}(R) \\ + \Delta\alpha_{mol}(R) \\ + \Delta\sigma_{IG}(R)n_{IG} \end{array} \right\} \end{array} \right\}$$

A
B
C
D
E
F

- Here, the Δ expressions consist of four terms each, but the outgoing laser wavelength terms are cancelled out

$$\Delta\xi = [\xi(\lambda_L) + \xi(\lambda_{RR})] - [\xi(\lambda_L) + \xi(\lambda_{VRR})] = \xi(\lambda_{RR}) - \xi(\lambda_{VRR})$$

with

$$\xi = \sigma_{abs}, \alpha_{aer}, \alpha_{mol}, \sigma_{IG}$$



Challenge in RVR Raman DIAL

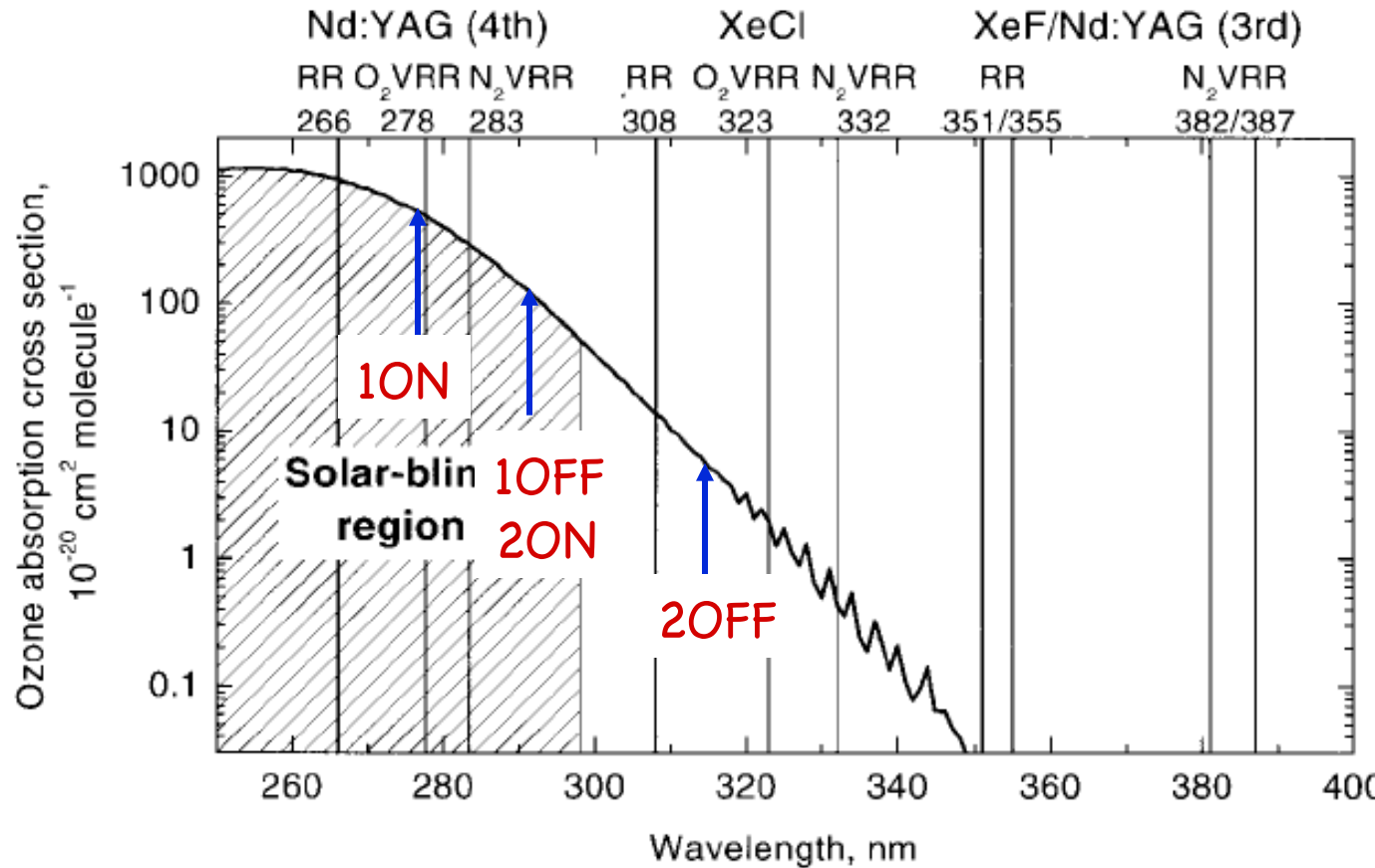
- ❑ Term B is range-independent, so the derivative is zero,
- ❑ Term C is only concerned about molecule Raman scattering.
- ❑ Term D will be determined through using the Raman VRR channel and introducing Angstrom exponent.
- ❑ Term E is concerned about molecule Rayleigh scattering, so can be calculated from atmosphere temperature and pressure.
- ❑ Term F can be minimized through choosing proper wavelengths, thus, can be ignored.

The main challenge in RVR Raman DIAL is how to sufficiently suppress the elastic scattering at laser wavelength in the pure rotational Raman (RR) channel, as the wavelength difference is only 1 nm.

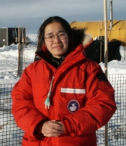
Modern interference filter has FWHM of 0.3 nm, but its wing (or tail) can certainly extend to more than 1 nm. Since Rayleigh scattering is about 3 orders of magnitude larger than rotational Raman scattering, the influence from Rayleigh scattering is not easy to be excluded. Thus, RVR Raman DIAL is not easy to be realized.



Multiwavelength (Raman) DIAL



Multiwavelength DIAL uses three or more wavelengths transmitted into the atmosphere and ozone is calculated from the differential absorption of several pairs of elastic scattering signals from air molecules and aerosols. The influence from differential scattering and extinction of aerosols are dramatically decreased by properly choosing wavelengths.



Multiwavelength DIAL Equation

□ For the elastic DIAL channel at 1ON-resonance wavelength,

$$P_S(\lambda_1^{ON}, R) = P_L(\lambda_1^{ON}) \left[(\beta_{aer}(\lambda_1^{ON}, R) + \beta_{mol}(\lambda_1^{ON}, R)) \Delta R \right] \left(\frac{A}{R^2} \right) \exp \left[-2 \int_0^R (\alpha_{aer}(\lambda_1^{ON}, r) + \alpha_{mol}(\lambda_1^{ON}, r)) dr \right]$$

$$\times \exp \left[-2 \int_0^R \sigma_{IG}(\lambda_1^{ON}, r) n_{IG}(r) dr \right] \exp \left[-2 \int_0^R \sigma_{abs}(\lambda_1^{ON}, r) n_c(r) dr \right] [\eta(\lambda_1^{ON}) G(R)] + P_B$$

□ For the elastic DIAL channel at 1OFF-resonance wavelength,

$$P_S(\lambda_1^{OFF}, R) = P_L(\lambda_1^{OFF}) \left[(\beta_{aer}(\lambda_1^{OFF}, R) + \beta_{mol}(\lambda_1^{OFF}, R)) \Delta R \right] \left(\frac{A}{R^2} \right) \exp \left[-2 \int_0^R (\alpha_{aer}(\lambda_1^{OFF}, r) + \alpha_{mol}(\lambda_1^{OFF}, r)) dr \right]$$

$$\times \exp \left[-2 \int_0^R \sigma_{IG}(\lambda_1^{OFF}, r) n_{IG}(r) dr \right] \exp \left[-2 \int_0^R \sigma_{abs}(\lambda_1^{OFF}, r) n_c(r) dr \right] [\eta(\lambda_1^{OFF}) G(R)] + P_B$$

□ For the elastic DIAL channel at 2ON-resonance wavelength,

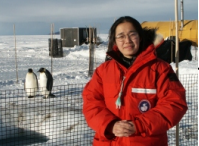
$$P_S(\lambda_2^{ON}, R) = P_L(\lambda_2^{ON}) \left[(\beta_{aer}(\lambda_2^{ON}, R) + \beta_{mol}(\lambda_2^{ON}, R)) \Delta R \right] \left(\frac{A}{R^2} \right) \exp \left[-2 \int_0^R (\alpha_{aer}(\lambda_2^{ON}, r) + \alpha_{mol}(\lambda_2^{ON}, r)) dr \right]$$

$$\times \exp \left[-2 \int_0^R \sigma_{IG}(\lambda_2^{ON}, r) n_{IG}(r) dr \right] \exp \left[-2 \int_0^R \sigma_{abs}(\lambda_2^{ON}, r) n_c(r) dr \right] [\eta(\lambda_2^{ON}) G(R)] + P_B$$

□ For the elastic DIAL channel at 2OFF-resonance wavelength,

$$P_S(\lambda_2^{OFF}, R) = P_L(\lambda_2^{OFF}) \left[(\beta_{aer}(\lambda_2^{OFF}, R) + \beta_{mol}(\lambda_2^{OFF}, R)) \Delta R \right] \left(\frac{A}{R^2} \right) \exp \left[-2 \int_0^R (\alpha_{aer}(\lambda_2^{OFF}, r) + \alpha_{mol}(\lambda_2^{OFF}, r)) dr \right]$$

$$\times \exp \left[-2 \int_0^R \sigma_{IG}(\lambda_2^{OFF}, r) n_{IG}(r) dr \right] \exp \left[-2 \int_0^R \sigma_{abs}(\lambda_2^{OFF}, r) n_c(r) dr \right] [\eta(\lambda_2^{OFF}) G(R)] + P_B$$



3-Wavelength Dual-DIAL for O_3

□ From above equations, we can derive the following

$$\begin{aligned}
 & \ln\left(\frac{P_S(\lambda_1^{ON}, R) - P_B}{P_S(\lambda_1^{OFF}, R) - P_B} \middle/ \frac{P_S(\lambda_2^{ON}, R) - P_B}{P_S(\lambda_2^{OFF}, R) - P_B}\right) = \ln\left(\frac{P_L(\lambda_1^{ON})\eta(\lambda_1^{ON})}{P_L(\lambda_1^{OFF})\eta(\lambda_1^{OFF})} \middle/ \frac{P_L(\lambda_2^{ON})\eta(\lambda_2^{ON})}{P_L(\lambda_2^{OFF})\eta(\lambda_2^{OFF})}\right) \\
 & + \ln\left(\frac{\beta_{aer}(\lambda_1^{ON}, R) + \beta_{mol}(\lambda_1^{ON}, R)}{\beta_{aer}(\lambda_1^{OFF}, R) + \beta_{mol}(\lambda_1^{OFF}, R)} \middle/ \frac{\beta_{aer}(\lambda_2^{ON}, R) + \beta_{mol}(\lambda_2^{ON}, R)}{\beta_{aer}(\lambda_2^{OFF}, R) + \beta_{mol}(\lambda_2^{OFF}, R)}\right) \\
 & - 2 \int_0^R \left[(\alpha_{aer}(\lambda_1^{ON}, r) - \alpha_{aer}(\lambda_1^{OFF}, r)) - (\alpha_{aer}(\lambda_2^{ON}, r) - \alpha_{aer}(\lambda_2^{OFF}, r)) \right] dr \\
 & - 2 \int_0^R \left[(\alpha_{mol}(\lambda_1^{ON}, r) - \alpha_{mol}(\lambda_1^{OFF}, r)) - (\alpha_{mol}(\lambda_2^{ON}, r) - \alpha_{mol}(\lambda_2^{OFF}, r)) \right] dr \\
 & - 2 \int_0^R \left[(\sigma_{IG}(\lambda_1^{ON}, r) - \sigma_{IG}(\lambda_1^{OFF}, r)) - (\sigma_{IG}(\lambda_2^{ON}, r) - \sigma_{IG}(\lambda_2^{OFF}, r)) \right] n_{IG}(r) dr \\
 & - 2 \int_0^R \left[(\sigma_{abs}(\lambda_1^{ON}, r) - \sigma_{abs}(\lambda_1^{OFF}, r)) - (\sigma_{abs}(\lambda_2^{ON}, r) - \sigma_{abs}(\lambda_2^{OFF}, r)) \right] n_c(r) dr
 \end{aligned}$$

Three wavelengths form a dual-pair DIAL, with $\lambda_{1OFF} = \lambda_{2ON}$. Thus, the influence from aerosol extinction and backscatter can be minimized by choosing appropriate pairs of wavelengths.



Solution for Dual-DIAL O_3

- ❑ Ozone number density can be derived from above equations:

$$n_c(R) = \frac{1}{2\Delta\sigma_{abs}} \frac{d}{dR} \left\{ \begin{array}{l} -\ln \left(\frac{P_S(\lambda_1^{ON}, R) - P_B}{P_S(\lambda_1^{OFF}, R) - P_B} \right) / \frac{P_S(\lambda_2^{ON}, R) - P_B}{P_S(\lambda_2^{OFF}, R) - P_B} \\ + \ln \left(\frac{P_L(\lambda_1^{ON})\eta(\lambda_1^{ON})}{P_L(\lambda_1^{OFF})\eta(\lambda_1^{OFF})} \right) / \frac{P_L(\lambda_2^{ON})\eta(\lambda_2^{ON})}{P_L(\lambda_2^{OFF})\eta(\lambda_2^{OFF})} \\ + \left[\ln \left(\frac{\beta_{aer}(\lambda_1^{ON}, R) + \beta_{mol}(\lambda_1^{ON}, R)}{\beta_{aer}(\lambda_1^{OFF}, R) + \beta_{mol}(\lambda_1^{OFF}, R)} \right) - \ln \left(\frac{\beta_{aer}(\lambda_2^{ON}, R) + \beta_{mol}(\lambda_2^{ON}, R)}{\beta_{aer}(\lambda_2^{OFF}, R) + \beta_{mol}(\lambda_2^{OFF}, R)} \right) \right] \end{array} \right\} A$$

$$- \frac{1}{\Delta\sigma_{abs}} \left\{ \begin{array}{l} \left[(\alpha_{aer}(\lambda_1^{ON}, R) - \alpha_{aer}(\lambda_1^{OFF}, R)) - (\alpha_{aer}(\lambda_2^{ON}, R) - \alpha_{aer}(\lambda_2^{OFF}, R)) \right] \\ + \left[(\alpha_{mol}(\lambda_1^{ON}, R) - \alpha_{mol}(\lambda_1^{OFF}, R)) - (\alpha_{mol}(\lambda_2^{ON}, R) - \alpha_{mol}(\lambda_2^{OFF}, R)) \right] \\ + \left[(\sigma_{IG}(\lambda_1^{ON}, R) - \sigma_{IG}(\lambda_1^{OFF}, R)) - (\sigma_{IG}(\lambda_2^{ON}, R) - \sigma_{IG}(\lambda_2^{OFF}, R)) \right] n_{IG}(R) \end{array} \right\} B$$

C

D

E

F

Where the differential absorption cross-section is defined as

$$\Delta\sigma_{abs} = \left(\sigma_{abs}(\lambda_1^{ON}, r) - \sigma_{abs}(\lambda_1^{OFF}, r) \right) - \left(\sigma_{abs}(\lambda_2^{ON}, r) - \sigma_{abs}(\lambda_2^{OFF}, r) \right)$$



Choice of Wavelength for Dual-DIAL

$$\Delta\beta = \ln\left(\frac{\beta_{aer}(\lambda_1^{ON}, R) + \beta_{mol}(\lambda_1^{ON}, R)}{\beta_{aer}(\lambda_1^{OFF}, R) + \beta_{mol}(\lambda_1^{OFF}, R)}\right) - \ln\left(\frac{\beta_{aer}(\lambda_2^{ON}, R) + \beta_{mol}(\lambda_2^{ON}, R)}{\beta_{aer}(\lambda_2^{OFF}, R) + \beta_{mol}(\lambda_2^{OFF}, R)}\right)$$

$$\Delta\alpha_{aer} = \left(\alpha_{aer}(\lambda_1^{ON}, R) - \alpha_{aer}(\lambda_1^{OFF}, R)\right) - \left(\alpha_{aer}(\lambda_2^{ON}, R) - \alpha_{aer}(\lambda_2^{OFF}, R)\right)$$

$$\Delta\alpha_{mol} = \left(\alpha_{mol}(\lambda_1^{ON}, R) - \alpha_{mol}(\lambda_1^{OFF}, R)\right) - \left(\alpha_{mol}(\lambda_2^{ON}, R) - \alpha_{mol}(\lambda_2^{OFF}, R)\right)$$

$$\Delta\sigma_{IG} = \left(\sigma_{IG}(\lambda_1^{ON}, R) - \sigma_{IG}(\lambda_1^{OFF}, R)\right) - \left(\sigma_{IG}(\lambda_2^{ON}, R) - \sigma_{IG}(\lambda_2^{OFF}, R)\right)$$

$$\Delta\sigma_{abs} = \left(\sigma_{abs}(\lambda_1^{ON}, r) - \sigma_{abs}(\lambda_1^{OFF}, r)\right) - \left(\sigma_{abs}(\lambda_2^{ON}, r) - \sigma_{abs}(\lambda_2^{OFF}, r)\right)$$

- Different channels interact on the same aerosols and interference gases (IG) but with different wavelengths. The main error in conventional DIAL is caused by the uncertainty of the wavelength dependence and information (like density) of the backscatter, extinction, and interference owing to aerosols and IG.

$$\beta_{aer}(\lambda) \propto \frac{1}{\lambda^a}, \quad \alpha_{aer}(\lambda) \propto \frac{1}{\lambda^a}$$

- If the wavelength dependence (Angstrom factor) is stable within the detection wavelength range, it is possible to cancel the influence by carefully choosing the wavelengths of two pairs – the difference between two pairs can be minimized.



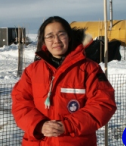
Solution for Dual-DIAL O₃

- ❑ By choosing the pairs of wavelengths, terms C-F (now the difference between two pairs of DIAL wavelengths) can be minimized or cancelled out. Thus, the O₃ measurement errors caused by the uncertainties of terms C-F can be dramatically decreased.
- ❑ Notice that the choice of the pairs of wavelengths must satisfy one important condition that the differential absorption cross-section given above must be large enough to meet the requirements of measurements sensitivity and spatial resolution.
- ❑ For the O₃ measurements, the dual-DIAL can be carried out by three wavelengths chosen at 277.1, 291.8, and 313.2 nm. The middle wavelength 291.8 nm acts as the off-wavelength for the 1st pair, while the on-wavelength for the 2nd pair.
- ❑ To minimize the influence from aerosol backscatter and extinction, a constant C can be introduced into above lidar equation. C is approximately determined by the ratio of the wavelength differences between two pairs of DIAL:

$$C = \frac{\lambda_1^{ON} - \lambda_1^{OFF}}{\lambda_2^{ON} - \lambda_2^{OFF}}$$

Here

$$\lambda_1^{OFF} = \lambda_2^{ON}$$



Solution with Constant C Introduced

$$n_c(R) = \frac{1}{2\Delta\sigma_{abs}} \frac{d}{dR} \left\{ \begin{array}{l} -\ln \left(\frac{P_S(\lambda_1^{ON}, R) - P_B}{P_S(\lambda_1^{OFF}, R) - P_B} \right) \left/ \left(\frac{P_S(\lambda_2^{ON}, R) - P_B}{P_S(\lambda_2^{OFF}, R) - P_B} \right)^C \right. \right) \\ + \ln \left(\frac{P_L(\lambda_1^{ON}) \eta(\lambda_1^{ON})}{P_L(\lambda_1^{OFF}) \eta(\lambda_1^{OFF})} \right) \left/ \left(\frac{P_L(\lambda_2^{ON}) \eta(\lambda_2^{ON})}{P_L(\lambda_2^{OFF}) \eta(\lambda_2^{OFF})} \right)^C \right. \right) \\ + \left[\ln \left(\frac{\beta_{aer}(\lambda_1^{ON}, R) + \beta_{mol}(\lambda_1^{ON}, R)}{\beta_{aer}(\lambda_1^{OFF}, R) + \beta_{mol}(\lambda_1^{OFF}, R)} \right) - C \ln \left(\frac{\beta_{aer}(\lambda_2^{ON}, R) + \beta_{mol}(\lambda_2^{ON}, R)}{\beta_{aer}(\lambda_2^{OFF}, R) + \beta_{mol}(\lambda_2^{OFF}, R)} \right) \right] \\ - \frac{1}{\Delta\sigma_{abs}} \left[\begin{array}{l} \left[(\alpha_{aer}(\lambda_1^{ON}, R) - \alpha_{aer}(\lambda_1^{OFF}, R)) - C(\alpha_{aer}(\lambda_2^{ON}, R) - \alpha_{aer}(\lambda_2^{OFF}, R)) \right] \\ + \left[(\alpha_{mol}(\lambda_1^{ON}, R) - \alpha_{mol}(\lambda_1^{OFF}, R)) - C(\alpha_{mol}(\lambda_2^{ON}, R) - \alpha_{mol}(\lambda_2^{OFF}, R)) \right] \\ + \left[(\sigma_{IG}(\lambda_1^{ON}, R) - \sigma_{IG}(\lambda_1^{OFF}, R)) - C(\sigma_{IG}(\lambda_2^{ON}, R) - \sigma_{IG}(\lambda_2^{OFF}, R)) \right] n_{IG}(R) \end{array} \right] \end{array} \right\}$$

A B C D E F

Where the differential absorption cross-section is defined as

$$\Delta\sigma_{abs} = \left(\sigma_{abs}(\lambda_1^{ON}, r) - \sigma_{abs}(\lambda_1^{OFF}, r) \right) - C \left(\sigma_{abs}(\lambda_2^{ON}, r) - \sigma_{abs}(\lambda_2^{OFF}, r) \right)$$

26



Simulation Results for Dual-DIAL O_3

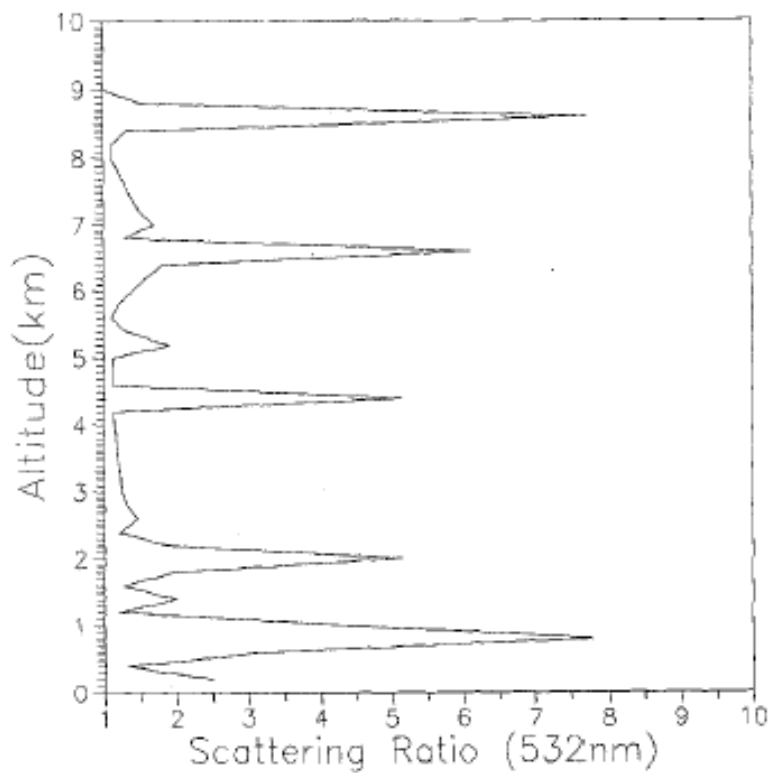


Fig. 1. Profile of the aerosol scattering ratio (532 nm)

$$C = 0.65$$

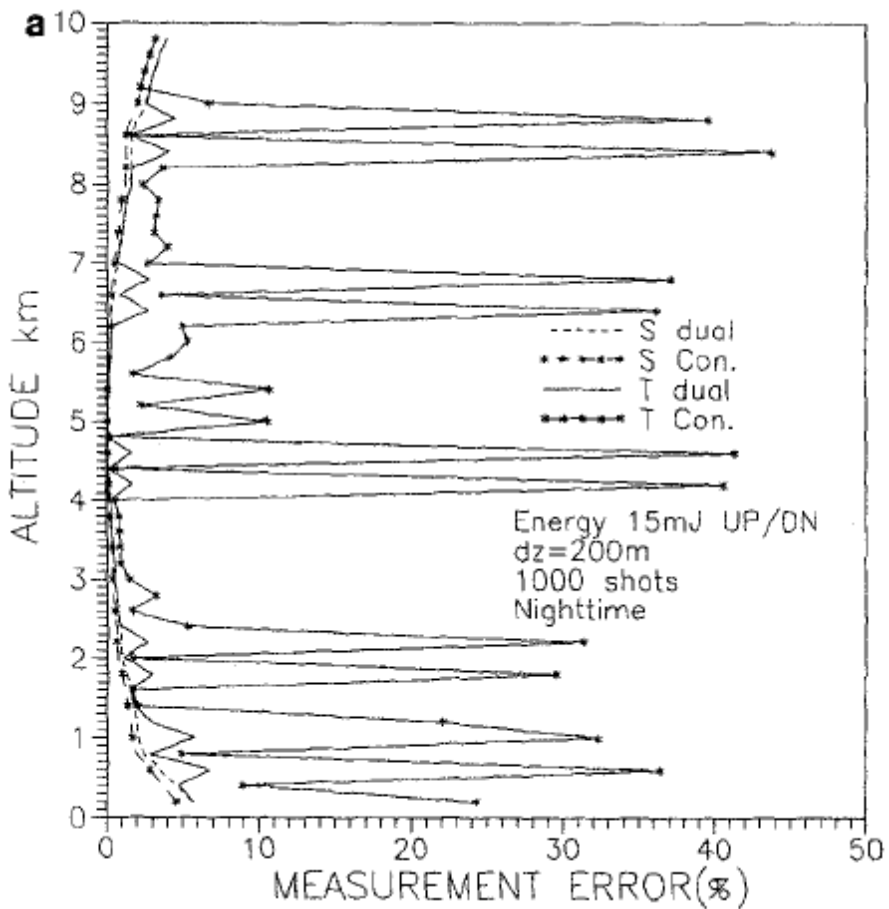


Fig. 2a, b. Simulations of measurement error vs altitude for the dual-DIAL with 277.1, 291.8, 313.2 nm and conventional DIAL with 277.1, 291.8 nm operated from an aircraft flying at an altitude of 5 km. The ozone profile is the US standard ozone profile. In the legend, S represents the statistical error, T the total measurement error, *dual* the dual-DIAL method and *con.* the conventional DIAL method: (a) night-time; (b) day-time



Dual-DIAL for SO_2 Measurements

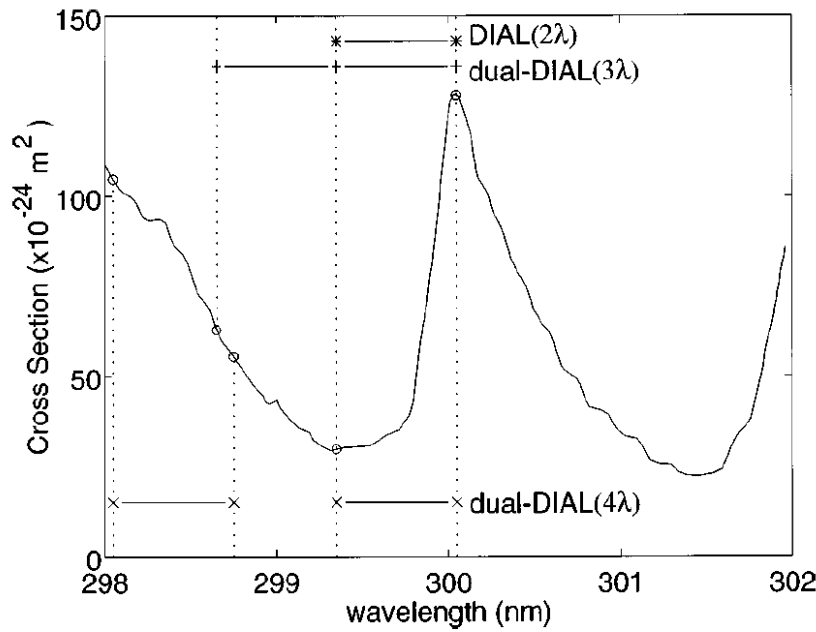


Fig. 1 Absorption cross section of SO_2 . The wavelengths used in two-wavelength DIAL, three-wavelength dual-DIAL, and four-wavelength dual-DIAL are indicated.

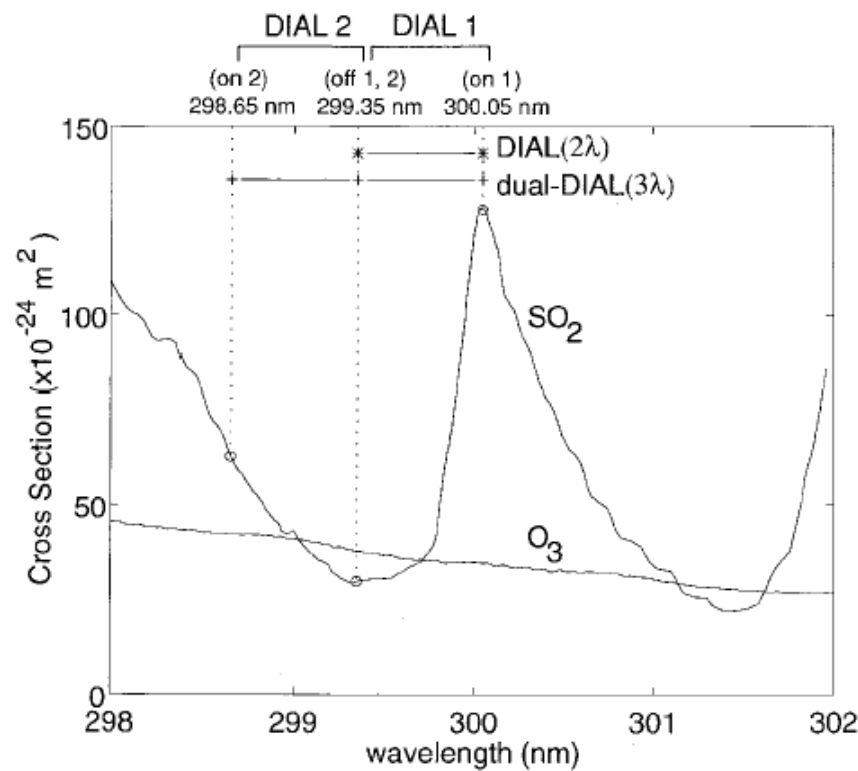


Fig. 1. Wavelengths used in three-wavelength dual DIAL for SO_2 , and absorption cross sections of SO_2 and O_3 .

Fukuchi et al., Opt. Eng., 38, 141-145, 1999
Fujii et al., Applied Optics, 40, 949-956, 2001



Dual-DIAL for SO₂ Measurements

Table 1 Cases considered for SO₂ measurement. $n\sigma'$ and $n\sigma''$ are given for a SO₂ concentration of 1 ppb.

Method	σ'_0, σ''_0 (10^{-24} m^2)	$n\sigma'_0, n\sigma''_0$ (10^{-6} m^{-1})	α'_x, α''_x (10^{-6} m^{-1})	i	λ_i (nm)	e_i
DIAL	98.0	2.5	−3.7	1	299.35	−1 ^a
				2	300.05	+1 ^b
Dual-DIAL:						
3-wavelength	131	3.3	0.83	1	298.65	+1
				2	299.35	−1
				3		
				4	300.05	+1
4-wavelength	148	3.8	0.094	1	298.05	+1
				2	298.75 299.35	−1
				3		
				4	300.05	+1

^aOff.

^bOn.

$$n = \frac{1}{2 \Delta R \sigma''_0} \left[\sum_{i=1}^m e_i Z(R, \lambda_i) - \sum_{i=1}^m e_i B(R, \lambda_i) \right] - \frac{\alpha''_x}{\sigma''_0},$$

$$\sigma''_0 = \sum_{i=1}^m e_i \sigma_0(\lambda_i)$$

$$\alpha''_x = \sum_{i=1}^m e_i \alpha_x(\lambda_i^{29})$$



Differential Optical Absorption Spectroscopy (DOAS)

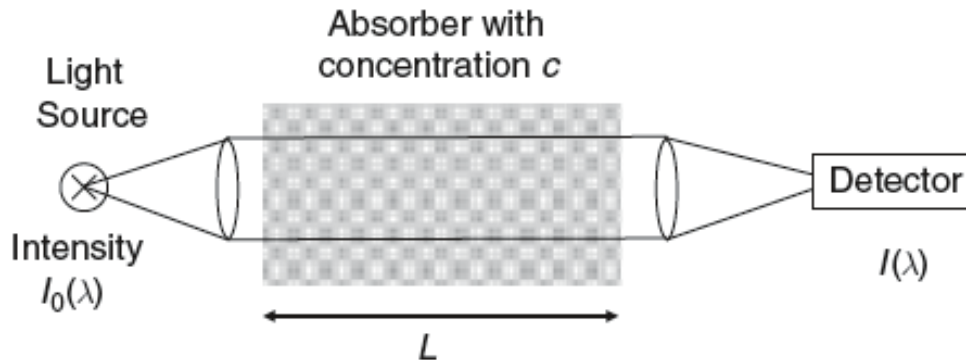
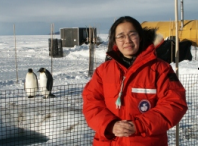


Fig. 6.1. The basic principle of absorption spectroscopic trace gas detection. A beam of light passes through a volume of length L containing the absorber with concentration c . At the end of the light path the intensity is measured by a suitable detector

$$dI(\lambda) = -I(\lambda)\alpha(\lambda)dz = -I\sigma_{ik}(\lambda)(N_i - N_k)dz$$

$$I(\lambda, z) = I_0 \exp \left[- \int_0^z \sigma_{ik}(\lambda)(N_i - N_k)dz \right] \rightarrow I(\lambda, z) = I_0 e^{-\sigma(\lambda)(N_i - N_k)L} = I_0 e^{-\alpha(\lambda)L}$$

-- Lambert-Beer's Law



DOAS Configurations

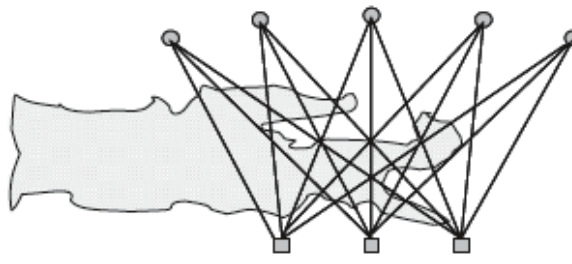
1. Long-Path DOAS (LP-DOAS)



2. Vertical Profiling LP-DOAS
Reflectors



3. Tomographic DOAS

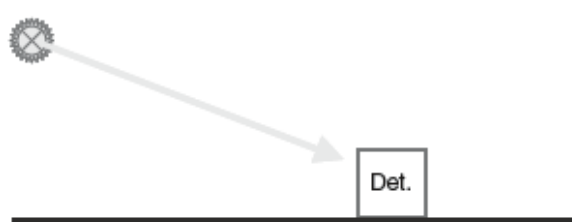


■ Light source
● Retro-reflector

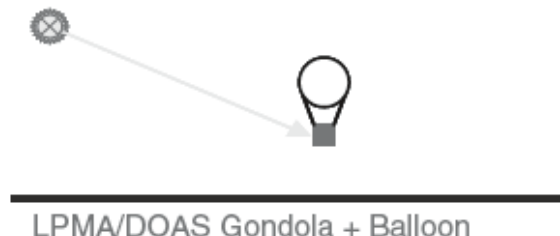
4. Folded-Path DOAS

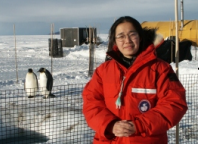


5. Direct Sunlight DOAS



6. Balloon-borne (direct sunlight) DOAS



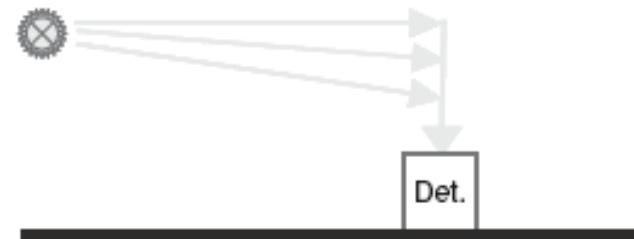


DOAS

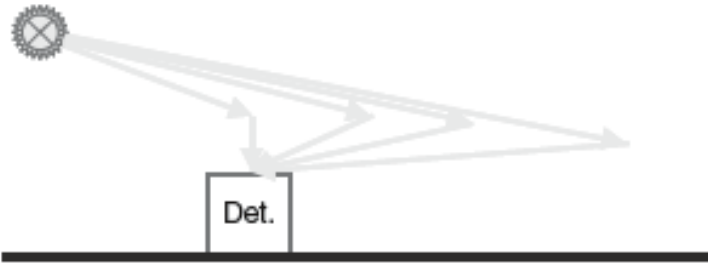
7. Satellite-borne DOAS - Occultation



8. Zenith Scattered Light (ZSL-DOAS)



9. Multi-Axis DOAS (MAX-DOAS)



10. Airborne Multi-Axis DOAS (AMAX-DOAS)

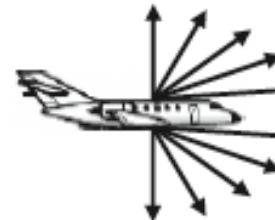
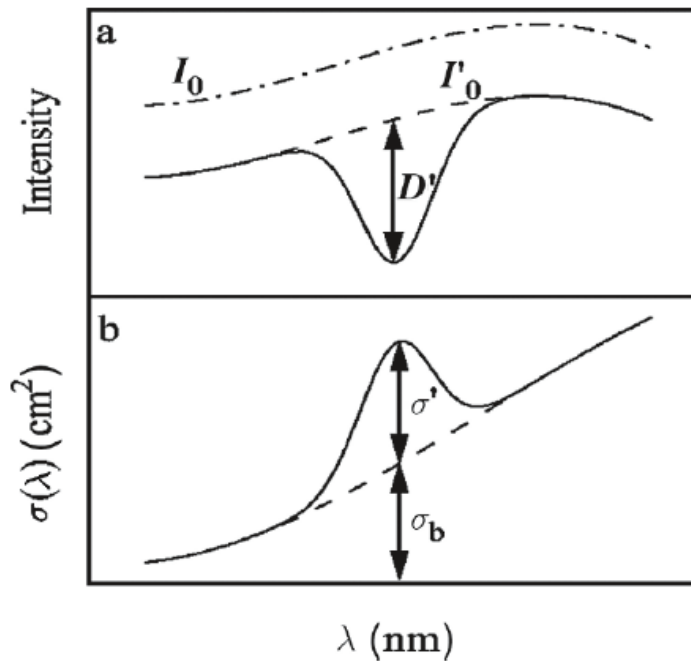


Fig. 6.4. The DOAS principle can be applied in a wide variety of light path arrangements and observation modes using artificial (1–4) as well as natural direct (5–7) or scattered (8–14) light sources. Measurements can be done from the ground, balloons, aircrafts, and from space



DOAS Principles



[Platt and Stutz,
DOAS Book, 2008]

Figure 6.3 illustrates the separation of the narrow- and broadband structures for one absorption band, both for the absorption cross-section and the intensity:

$$\sigma_j(\lambda) = \sigma_{j0}(\lambda) + \sigma'_j(\lambda) \quad (6.5)$$

σ_{j0} in (6.5) varies ‘slowly’ with the wavelength λ , for instance describing a general ‘slope’, such as that caused by Rayleigh and Mie scattering, while $\sigma'_j(\lambda)$ shows rapid variations with λ , for instance due to an absorption band (see Fig. 6.3). The meaning of ‘rapid’ and ‘slow’ variation of the absorption cross-section as a function of wavelength is, of course, a question of the observed wavelength interval and the width of the absorption bands to be detected.



DOAS Principles

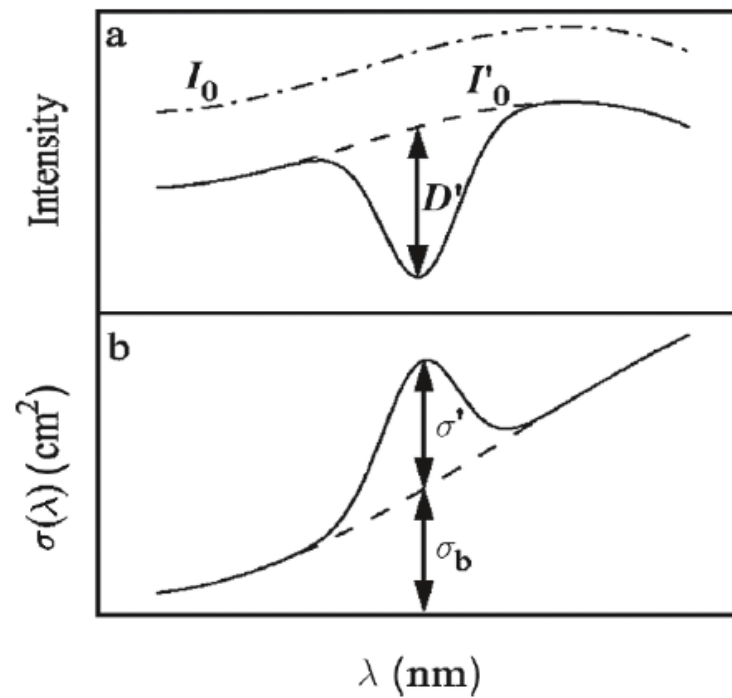
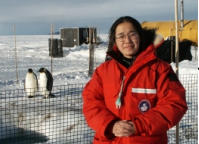
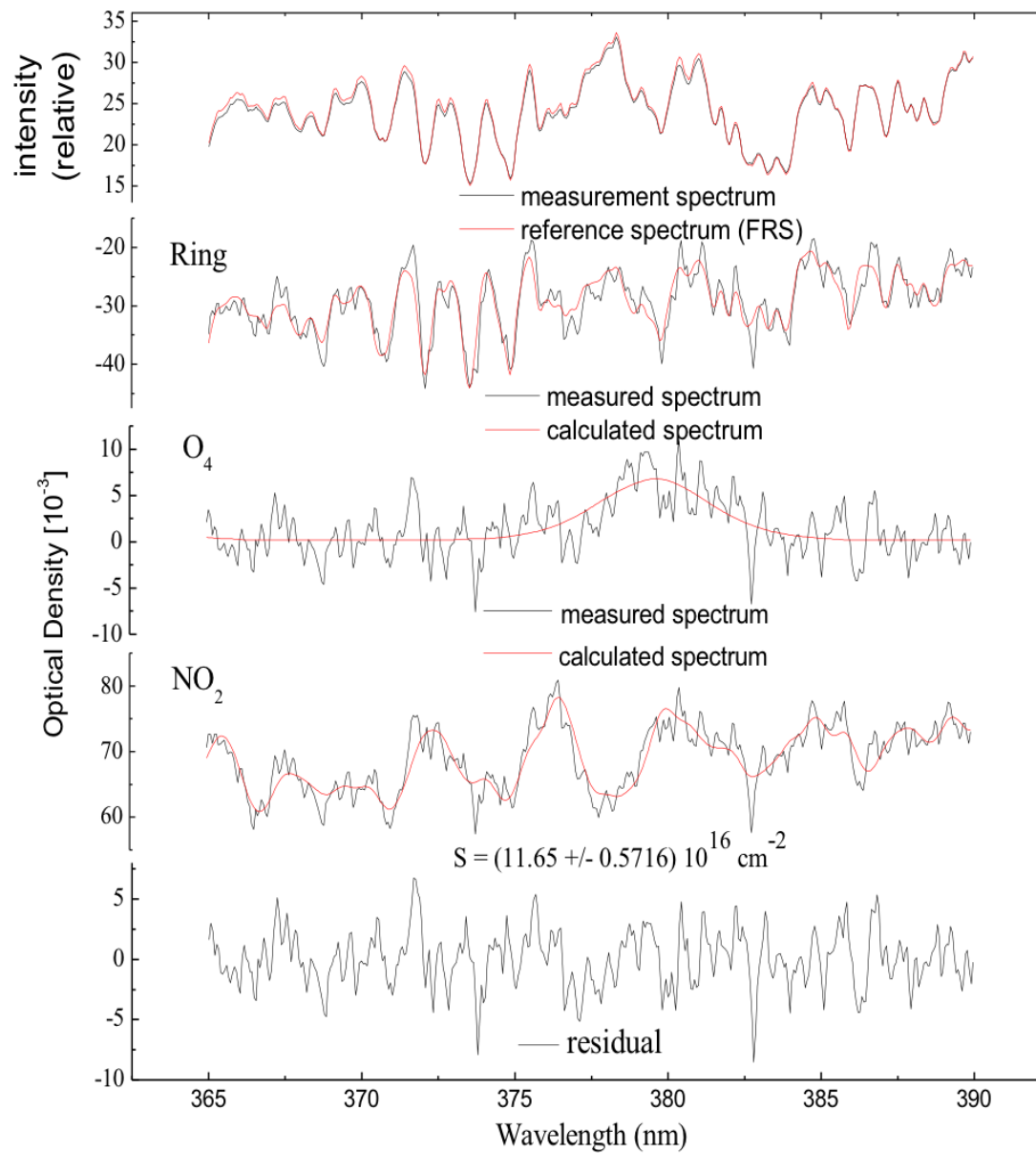


Fig. 6.3. Principle of DOAS: I_0 and σ are separated by an adequate filtering procedure into a narrow (D' , and σ') and broad band part (I'_0 and σ_b)

$$\begin{aligned} I(\lambda) = I_0(\lambda) \cdot \exp \left[-L \cdot \left(\sum_j (\sigma'_j(\lambda) \cdot c_j) \right) \right] \cdot \\ \exp \left[-L \cdot \left(\sum_j (\sigma_{j0}(\lambda) \cdot c_j) + \varepsilon_R(\lambda) + \varepsilon_M(\lambda) \right) \right] \cdot A(\lambda) \end{aligned}$$



DOAS Principles





DOAS Principles

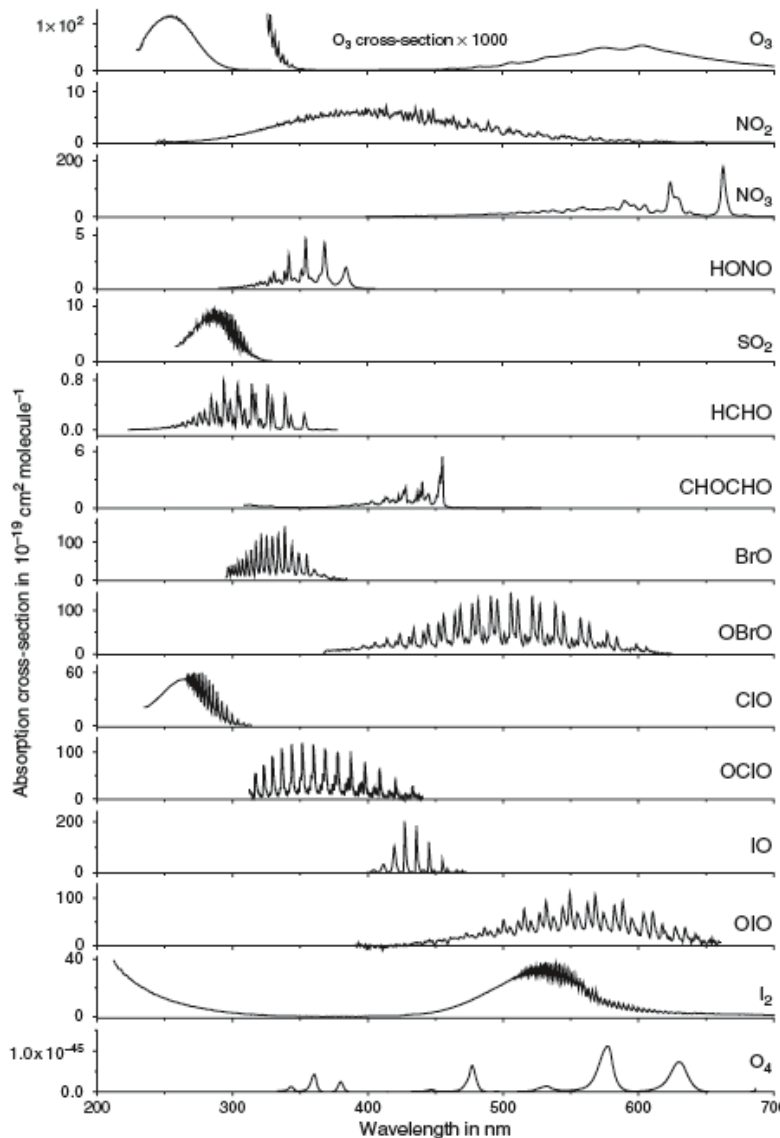


Fig. 6.5. Details of the absorption cross-section features of a number of species of atmospheric interest as a function of wavelength (in nm). Note the 'fingerprint' nature of the different spectra

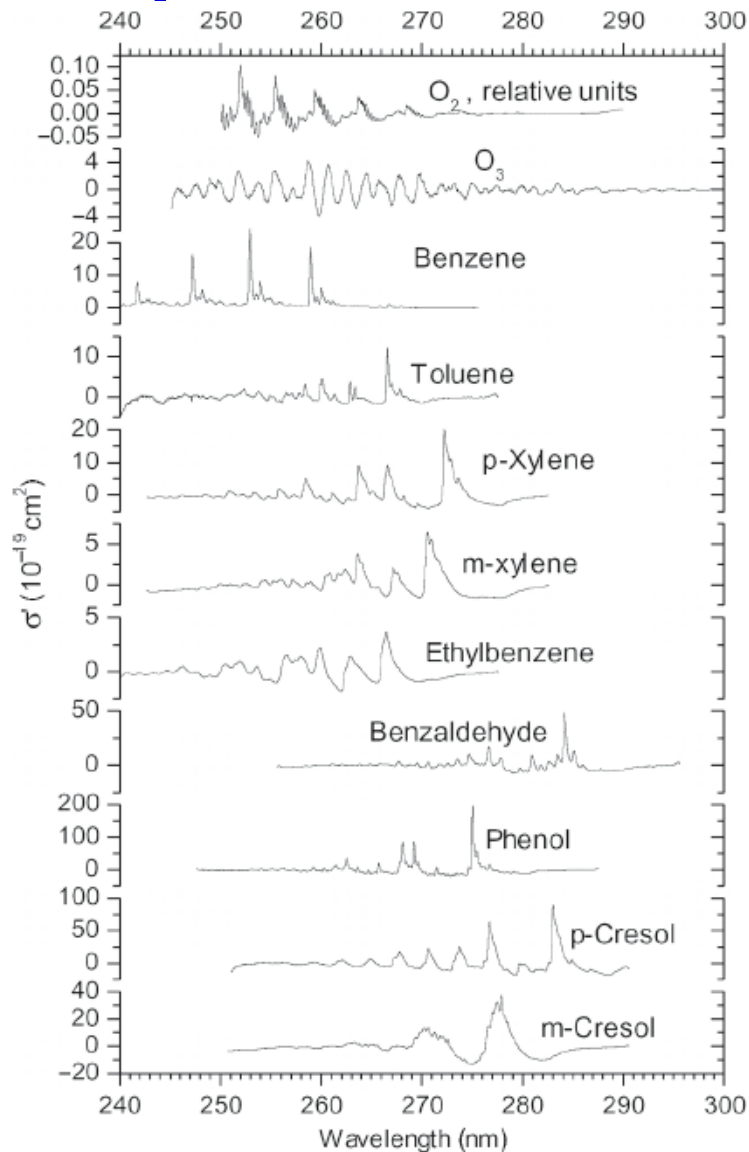


Fig. 6.6. Details of the differential absorption cross-section features of a number of monocyclic aromatic species, O₂, and O₃ as a function of wavelength (in nm). Note the 'fingerprint' nature of the different spectra



MAX-DOAS Principles

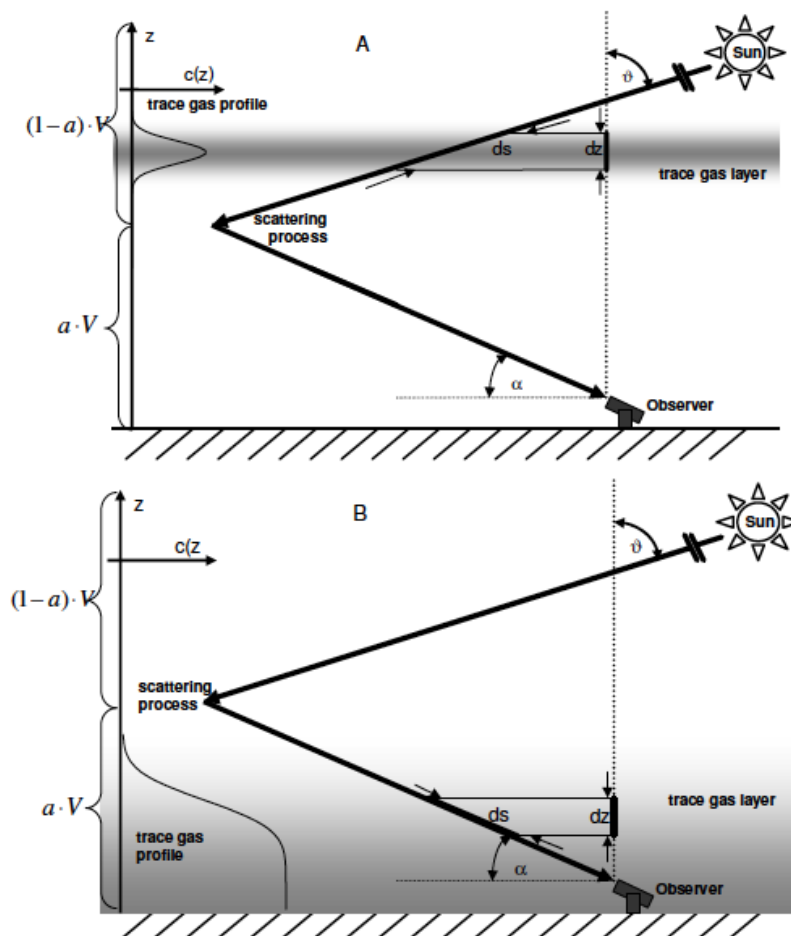


Fig. 1. Observation geometries for ground based DOAS using scattered sunlight: Light enters the atmosphere at a certain solar zenith angle ϑ . In the single scattering approximation light received by the observer was scattered exactly once into the telescope viewing direction defined by the observation elevation angle α . The observed SCD (integral along ds) is larger than the VCD (integral along dz), with AMF being the conversion factor. Panel A represents the situation for a high (stratospheric) trace gas layer, panel B is representative for a trace gas layer near the surface.

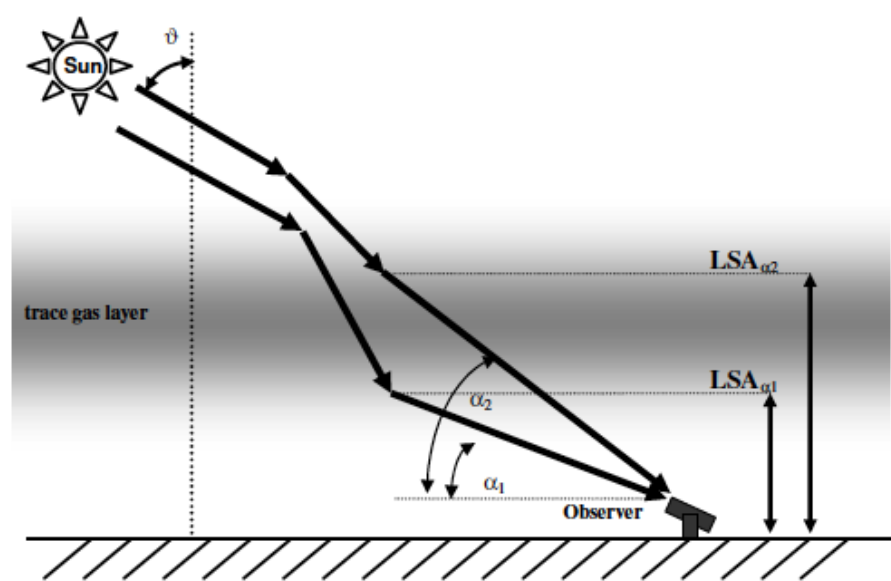


Fig. 5. The Last Scattering Altitude LSA: for low elevation angles, the mean free path in the viewing direction is shorter due to higher density and/or aerosol load. This can result in the slant path through absorbing layers at higher altitudes being shorter for lower elevation angles than for higher ones.

[Hönniger et al., ACP, 2004]



MAX-DOAS Principles

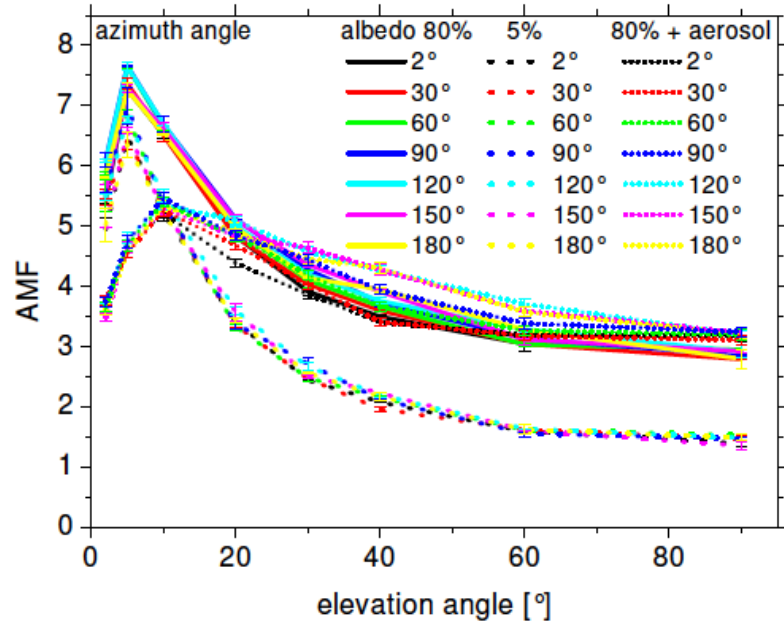


Fig. 11. Azimuth-dependence of the AMF for 30° SZA and profile P4 (trace gas layer at 1–2 km altitude). For relative azimuth angles between 2° (looking almost towards the sun) and 180° (looking away from the sun) only a small effect increasing with ground albedo and aerosol load can be seen. Calculations were performed for a ground albedo of 80% and 5% (cf. Fig. 3) in the Rayleigh case (in the troposphere) and for 80% ground albedo in the low aerosol case (cf. Fig. 4).

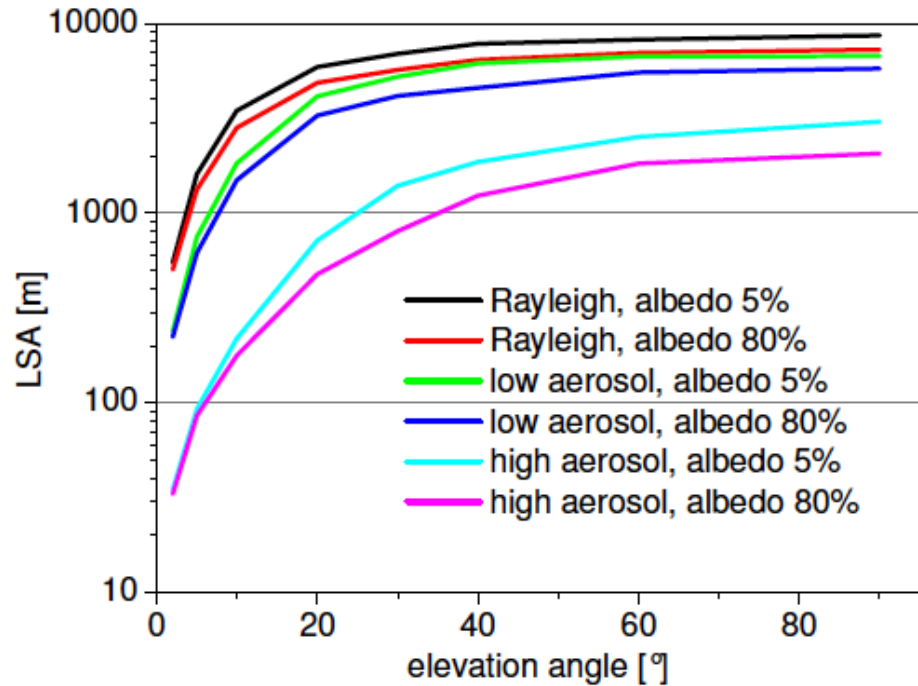


Fig. 8. Last scattering altitude (LSA) for pure Rayleigh, low and high aerosol load scenarios (see Fig. 4) and both, 5% and 80% albedo. The LSA is generally below 1km for the lowest elevation angle and above 1km for the highest elevation angles, especially for zenith viewing direction.

[Hönniger et al., ACP, 2004]



MAX-DOAS Measurements

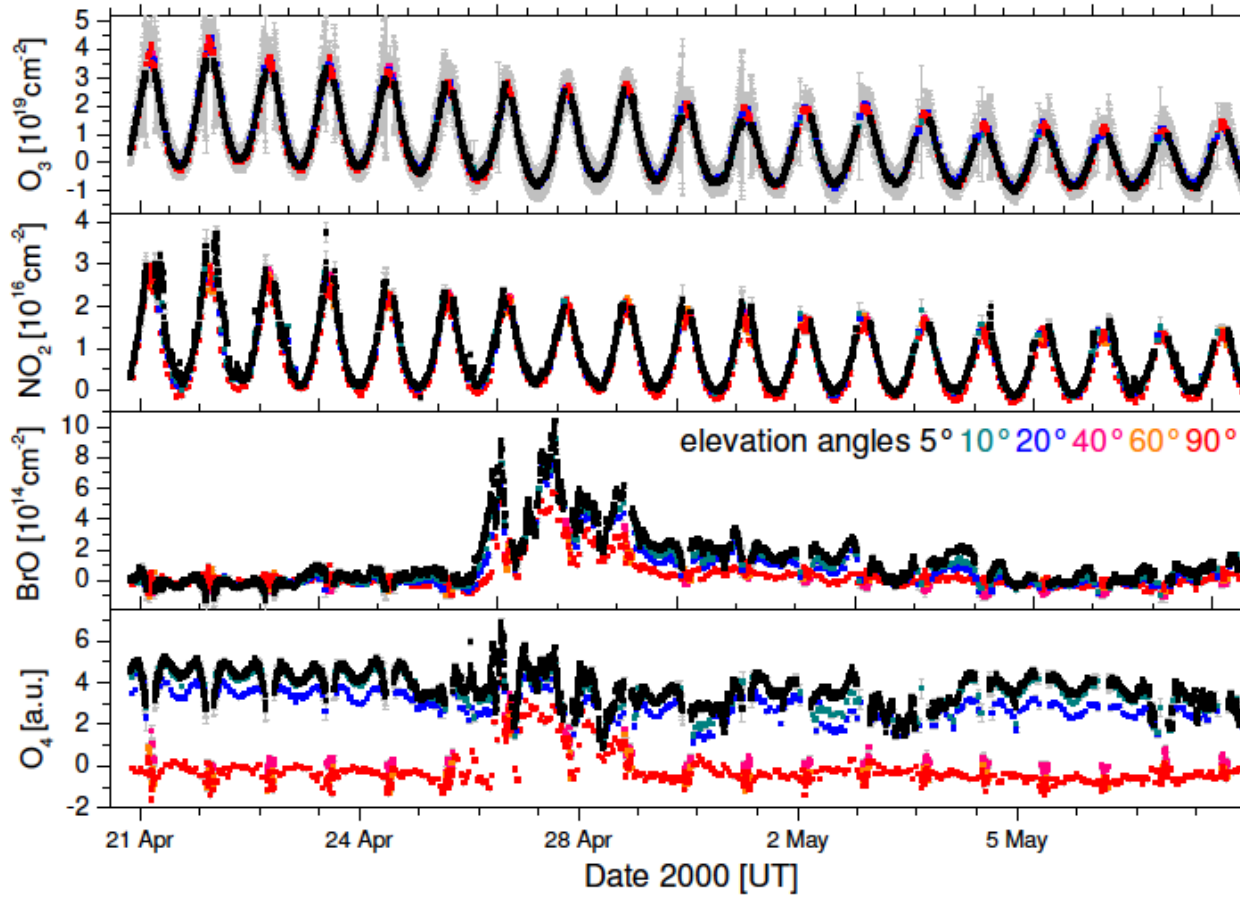


Fig. 18. MAX-DOAS time series of DSCD's of O_3 , NO_2 , O_4 and BrO at Alert during spring of 2000. Error bars (2σ) are shown in light grey. The O_3 and NO_2 columns show no variation for the different elevation angles indicating that the bulk of these species is located in the stratosphere. In contrast to that the O_4 data vary strongly with elevation angle. Enhanced O_4 levels around 27/28 April at high elevation angles indicate periods of snowdrift. Following 27 April the BrO columns show strong differences for different elevation angles due to BrO presence in the boundary layer. Effects of snowdrift on 27/28 April can be seen like for O_4 .

[Hönniger et al., ACP, 2004]



MAX-DOAS Measurements

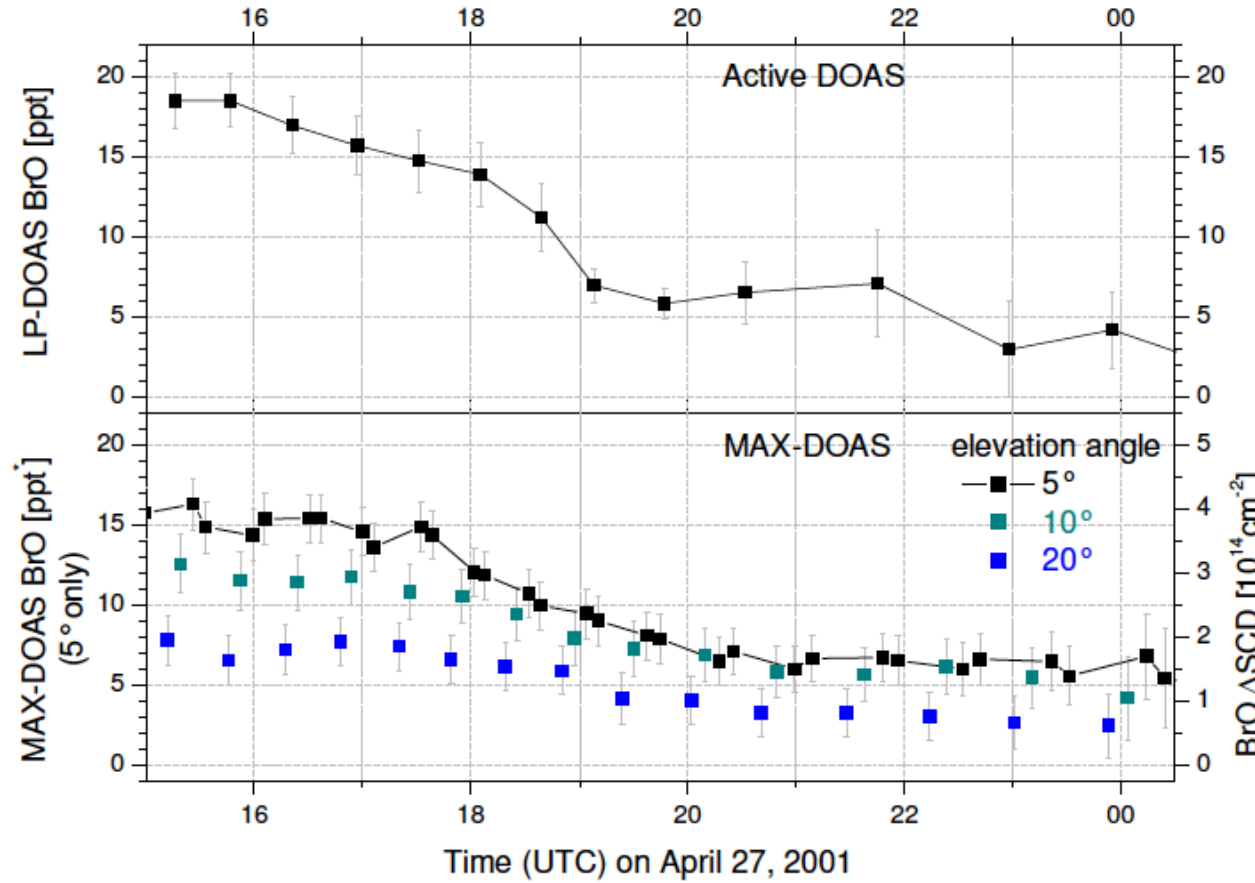
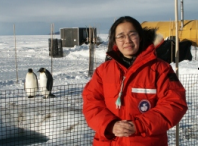
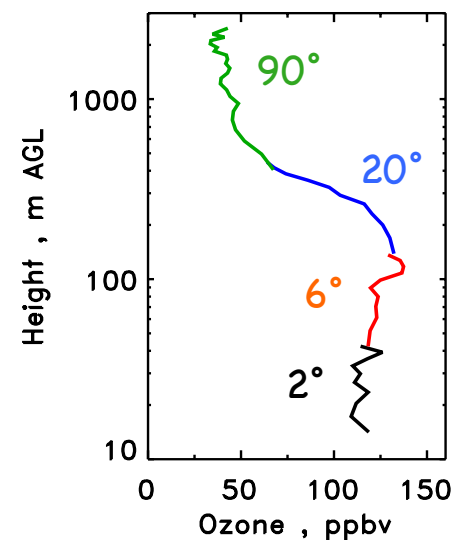
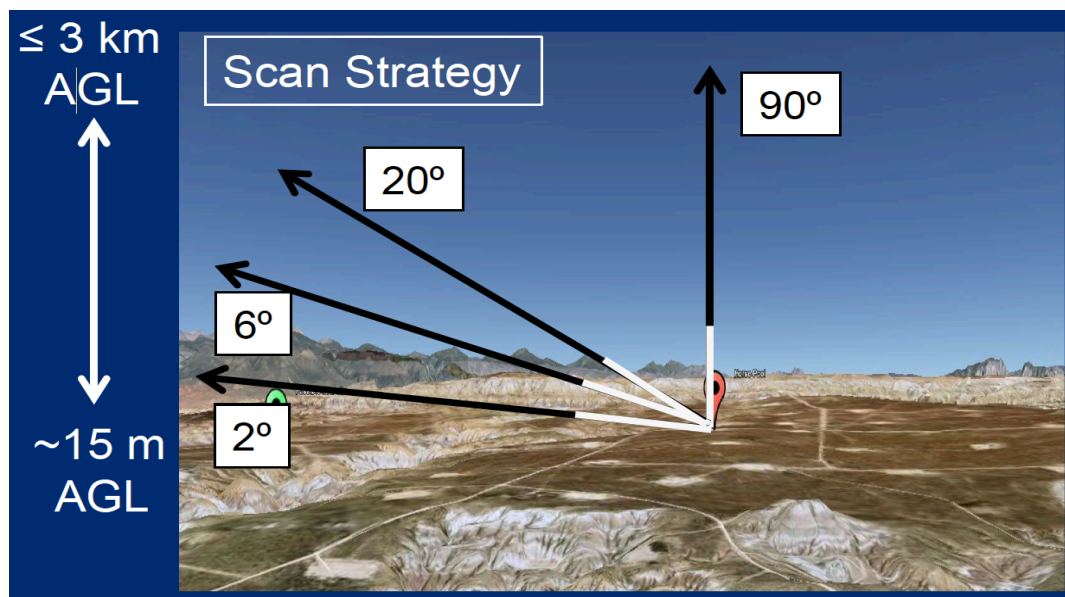


Fig. 21. Comparison of active long path DOAS and passive MAX-DOAS BrO measurements at the Hudson Bay for 27 April 2001. From the elevation angle dependence of the Δ SCD's a ~ 1 km BrO layer at the surface can be concluded for e.g. 16:00 h. Using this layer thickness the 5° BrO Δ SCD's were converted to mixing ratios for better comparison with the long path DOAS data (Hönniger et al., 2003a).

[Hönniger et al., ACP, 2004]



Multi-Angle Pointing TOPAZ Lidar



Composite vertical O_3 and aerosol profiles every 5 min

[Courtesy of Dr. Chris Senff]